Electronic Research Archive

https://www.aimspress.com/journal/era

ERA, 34(6): 4051–4079.
DOI: 10.3934/era.2026182
Received: 16 March 2026
Revised: 27 April 2026
Accepted: 08 May 2026
Published: 15 May 2026

Research article

Fault-resilient output-feedback control of delayed memristor-based neural networks with dual performance guarantees

Qinru Yang*

School of Computer Science and Technology, Anhui University of Technology, Ma'anshan 243032, China

* **Correspondence:** Email: yangqinru@ahut.edu.cn.

Abstract: This work investigated the fault-resilient output-feedback control problem for delayed memristor-based neural networks (MBNNs) subject to actuator faults and external disturbances. To overcome the practical limitation that full-state measurements are often unavailable, an output-feedback controller was designed to rely solely on measurable outputs. By constructing a Lyapunov-Krasovskii functional and employing the Bessel-Legendre inequality together with the generalized reciprocally convex combination inequality, a sufficient condition was established to simultaneously guarantee $\mathcal{H}_\infty$ and $\mathcal{L}_2 - \mathcal{L}_\infty$ disturbance attenuation for the considered MBNNs. Decoupling techniques were then introduced to eliminate nonlinear coupling terms, and the controller synthesis was formulated in terms of linear matrix inequalities that are solvable with existing convex optimization tools. Finally, a numerical example was provided to corroborate the reduced conservatism of the proposed analysis condition and the effectiveness of the synthesis method in achieving the desired dual-performance guarantees.

Keywords: memristor-based neural network; fault-resilient control; output-feedback control; $\mathcal{H}_\infty$ performance; $\mathcal{L}_2 - \mathcal{L}_\infty$ performance

1. Introduction

Over the past few years, delayed memristor-based neural networks (MBNNs), a special class of recurrent neural networks (NNs) [1], have attracted increasing research attention due to their distinctive nonlinear characteristics [2, 3], memory-dependent dynamics [4], and hardware-friendly implementation [5]. By incorporating memristive synaptic weights into recurrent NN architectures, such systems can effectively model complex biological learning behaviors and exhibit rich dynamic phenomena, including multistability [6], chaos [7], and state-dependent switching dynamics [8]. These features enable wide-ranging applications in areas such as associative memory [9], image segmentation [10], pattern recognition [11], secure communications [12], and neuromorphic computing [13]. The dynamic behaviors of delayed MBNNs play a fundamental role in these applications. Consequently, quantitative

analysis and control synthesis for delayed MBNNs have become important research topics, and a growing body of literature in recent years has reported significant theoretical and methodological advances in this area [14–18].

In real-world dynamical systems, external disturbances are unavoidable due to practical operating conditions. To mitigate their adverse effects, various robust control strategies with disturbance attenuation capabilities have been developed. Yan et al. [19] established stabilization criteria for delayed memristive NNs via sampled-data control with quantization. In parallel, Lin et al. [20] explored $\mathcal{H}_\infty$ synchronization for coupled memristive NNs featuring reaction-diffusion terms and delays with both state and spatial diffusion coupling. By contrast, Huang and Li [21] studied derivative-coupled delayed memristive NNs and introduced the notions of general decay $\mathcal{H}_\infty$ anti-synchronization grounded in ψ-type stability, thereby enabling explicit convergence-rate characterization within an anti-synchronization framework. The $\mathcal{H}_\infty$ performance bounds the induced $\mathcal{L}_2$ gain from disturbance to output, reflecting energy-to-energy attenuation. Meanwhile, the $\mathcal{L}_2 - \mathcal{L}_\infty$ performance limits the peak response, providing an energy-to-peak robustness measure. Wang et al. [22] addressed the finite-time $\mathcal{L}_2 - \mathcal{L}_\infty$ synchronization analysis for inertial NNs with semi-Markov jumps via sampled-data control, where the time-varying delay is piecewise differentiable. In a related study, Wang and Zhu [23] investigated memristive NNs experiencing time-dependent delays that do not strictly require differentiability and established an $\mathcal{L}_2 - \mathcal{L}_\infty$ stability criterion via a suitably constructed Lyapunov-Krasovskii functional (LKF). Most of the aforementioned studies are based on state-feedback control strategies, which rely on the full availability of neuron states. In a practical system, full-state measurements are either unavailable or difficult to obtain accurately due to limited accessibility, communication constraints, or measurement noise [24]. By contrast, output-feedback control, which only utilizes measurable outputs for controller design, is more favorable for implementation. This motivates the investigation of disturbance attenuation control strategies for MBNNs based on output feedback.

From another practical standpoint, actuator faults are ubiquitous in many control systems due to component aging, hardware degradation, and harsh operating environments, potentially leading to performance degradation, instability, or even catastrophic system damage [25–27]. To mitigate such adverse effects, fault-resilient control strategies have been extensively scrutinized over the past few years [28–32]. It has been shown that appropriately designed fault-resilient controllers can compensate for fault effects, preserve system stability, and recover system performance to a desired level, thereby ensuring reliable system operation under unexpected actuator malfunctions. Representative studies cover diverse systems: Liu and Dong [33] proposed a privacy-preserving hierarchical control framework for heterogeneous multi-agent systems under actuator faults. Du et al. [34] addressed asymmetric wing damage in fixed-wing aircraft via an integrated scheme of extended state observation, dynamic regressor extension and mixing, and adaptive control allocation. Furthermore, Jamali et al. [35] developed a distributed finite-time fault-resilient control strategy for isolated AC microgrids. Regarding dynamic NNs, Zhou et al. [36] investigated anti-synchronization for stochastic delayed reaction–diffusion NNs and proposed a fault-resilient controller design strategy, Chen et al. [37] examined synchronization of uncertain quaternion-valued NNs via a fault-resilient dual-controller scheme, and Radhika et al. [38] presented a fault-resilient state estimation method for competitive NNs using high-order integral LKFs. Despite these advancements, research on fault-resilient control for delayed MBNNs remains relatively scarce, particularly in the context of output-feedback design.

Inspired by the preceding discussions, this research focuses on addressing the fault-resilient output-

feedback control problem for delayed MBNNs subject to actuator faults and external disturbances. The main contributions of this paper can be summarized as follows:

1) An output-feedback control scheme is presented for delayed MBNNs subject to actuator faults and external disturbances. Unlike existing works relying on full-state measurements (e.g., [19–21]), the present scheme only utilizes measurable outputs, which makes it more practical for real-world applications with limited state accessibility. Furthermore, in contrast to single-performance studies [22, 23], the proposed scheme simultaneously guarantees both $\mathcal{H}_\infty$ and $\mathcal{L}_2 - \mathcal{L}_\infty$ disturbance attenuation, providing a more comprehensive robustness characterization.

2) Two conditions for analysis and controller synthesis of the considered MBNNs are successively derived. By employing the Bessel-Legendre inequality (BLI) and the generalized reciprocally convex combination inequality (GRCCI), the approximation errors during the bounding process of integral terms are reduced. Numerical results confirm that the proposed analysis condition yields larger allowable upper delay bounds than those reported in [19, 23, 39], even under more stringent dual-performance requirements.

The rest of this paper is organized as follows. Section 2 introduces the delayed MBNN model, actuator fault description, uncertain system transformation, and the required preliminaries. Section 3 presents a condition for the dual $\mathcal{H}_\infty$ and $\mathcal{L}_2 - \mathcal{L}_\infty$ performance analysis by constructing an LKF and employing the BLI and GRCCI. Section 4 develops a synthesis condition using several decoupling techniques to eliminate nonlinear coupling terms. Section 5 provides a numerical example to corroborate the reduced conservatism of the proposed analysis condition and the effectiveness of the synthesis method in achieving the desired dual-performance guarantees. Finally, Section 6 concludes the paper and discusses possible future research directions.

2. Preliminaries

This section describes the delayed MBNN model and actuator failures, outlines the process of uncertain system transformation, presents the performance definitions, assumption, and key lemmas, and details the fault-resilient output-feedback control problem under investigation. The notations used in this and subsequent sections conform to those outlined in [40–42], except where otherwise specified.

2.1. System model and actuator failure description

The model for the time-delayed MBNN under investigation is established as

$$\begin{aligned} \dot{\eta}(t) &= -D\eta(t) + A(\eta(t))\varsigma(\eta(t)) + A_d(\eta(t))\varsigma(\eta(t-\rho(t))) + Bu^f(t) + Ew(t), \\ y(t) &= C\eta(t), \end{aligned} \tag{2.1}$$

where the vector $\eta(t) = \text{col}\{\eta_1(t), \eta_2(t), \ldots, \eta_n(t)\} \in \mathbb{R}^n$ represents the neural state, $y(t) \in \mathbb{R}^p$ the measurable system output, and $\rho(t)$ a bounded time-dependent delay such that $\rho(t) \in [\rho_1, \rho_2]$, with ρ_1 and ρ_2 being constants. The nonlinear activation function is expressed by $\varsigma(\cdot) = \text{col}\{\varsigma_1(\cdot), \varsigma_2(\cdot), \ldots, \varsigma_n(\cdot)\} \in \mathbb{R}^n$, and it satisfies $\varsigma_k(0) = 0$ for all $k = 1, 2, \ldots, n$ [43]. The matrix $D = \text{diag}\{d_1, d_2, \ldots, d_n\}$ denotes a positive diagonal matrix characterizing self-feedback. Meanwhile, $A(\eta(t)) = (a_{ij}(\eta_i(t)))_{n\times n}$ and $A_d(\eta(t)) = (a_{dij}(\eta_i(t)))_{n\times n}$ describe the memristive coupling weights for the current-state and delayed-state channels, respectively. In addition, $w(t) \in \mathbb{R}^q$ stands for the disturbance input and is assumed to lie in $L_2[0, \infty)$. The matrices $B \in \mathbb{R}^{n\times m}$, $C \in \mathbb{R}^{p\times n}$, and $E \in \mathbb{R}^{n\times q}$ are known and dimensionally compatible.

Following [36], the actuator failure model is described as

$$u^f(t) = (F_0 + F_1\lambda)u(t), \quad |\lambda| \le I,$$

where F_0, F_1, and λ are defined as

$$\begin{aligned} F_0 &= \operatorname{diag}\left\{(\hat{f}_1 + \check{f}_1)/2, \ldots, (\hat{f}_m + \check{f}_m)/2\right\}, \\ F_1 &= \operatorname{diag}\left\{(\hat{f}_1 - \check{f}_1)/2, \ldots, (\hat{f}_m - \check{f}_m)/2\right\}, \\ \lambda &= \operatorname{diag}\{\lambda_1, \lambda_2, \ldots, \lambda_m\} \end{aligned}$$

with $0 \le \check{f}_k \le f_k \le \hat{f}_k$, $k \in \{1, \ldots, m\}$. Here, $u^f(t)$ denotes the actual control input applied to the plant after actuator degradation, while $u(t)$ is the nominal control input generated by the controller. The diagonal matrix F_0 represents the nominal effectiveness level of each actuator, and F_1 characterizes the admissible variation range of actuator effectiveness. The uncertain diagonal matrix λ describes time-varying fault factors satisfying $|\lambda| \le I$. For each actuator channel k, $\check{f}_k$ and $\hat{f}_k$ denote the lower and upper bounds of the corresponding effectiveness coefficient, respectively.

In contrast to most existing control strategies, such as the event-triggered impulsive control in [44], the intermittent control in [45], and the bumpless transfer control in [46], which rely on state-feedback, this work aims to develop an output-feedback control law of the form

$$u(t) = Ky(t), \tag{2.2}$$

where $u(t) \in \mathbb{R}^m$ denotes the control input and $K \in \mathbb{R}^{m\times p}$ is the output-feedback gain matrix to be designed.

2.2. Uncertain system transformation

Throughout this paper, the memristive connection weights in the MBNN system (2.1) are assumed to obey piecewise constant switching rules determined by the neuron states, namely,

$$a_{ij}(\eta_i(t)) = \begin{cases} \check{a}_{ij}, & |\eta_i(t)| \le \vartheta_i, \\ \hat{a}_{ij}, & |\eta_i(t)| > \vartheta_i, \end{cases} \quad i, j \in \iota,$$

$$a_{dij}(\eta_i(t)) = \begin{cases} \check{a}_{dij}, & |\eta_i(t)| \le \vartheta_i, \\ \hat{a}_{dij}, & |\eta_i(t)| > \vartheta_i, \end{cases} \quad i, j \in \iota,$$

where $\vartheta_i > 0$ is the switching threshold, and $\check{a}_{ij}, \hat{a}_{ij}, \check{a}_{dij}$, and $\hat{a}_{dij}$ are prescribed constants.

Since the memristive weights depend explicitly on the system states, system (2.1) is essentially a state-dependent switching system. In light of the Filippov theory for differential equations with discontinuous right-hand sides, the memristive weights can be described by set-valued maps and differential inclusions. Based on this formulation, the state-dependent switching terms can be further transformed into an equivalent uncertain system representation. To facilitate the subsequent analysis, we introduce the following auxiliary functions:

$$\Xi^a_{ij}(\eta_i(t)) = \begin{cases} \operatorname{sign}(\check{a}_{ij} - \hat{a}_{ij}), & |\eta_i(t)| \le \vartheta_i, \\ -\operatorname{sign}(\check{a}_{ij} - \hat{a}_{ij}), & |\eta_i(t)| > \vartheta_i, \end{cases}$$

$$\Xi^b_{ij}(\eta_i(t)) = \begin{cases} \operatorname{sign}(\check{a}_{dij} - \hat{a}_{dij}), & |\eta_i(t)| \le \vartheta_i, \\ -\operatorname{sign}(\check{a}_{dij} - \hat{a}_{dij}), & |\eta_i(t)| > \vartheta_i. \end{cases}$$

Accordingly, the memristive weights can be equivalently expressed as

$$a_{ij}(\eta_i(t)) = \frac{\check{a}_{ij} + \hat{a}_{ij}}{2} + \frac{\check{a}_{ij} - \hat{a}_{ij}}{2}\,\Xi^a_{ij}(\eta_i(t)),$$

$$a_{dij}(\eta_i(t)) = \frac{\check{a}_{dij} + \hat{a}_{dij}}{2} + \frac{\check{a}_{dij} - \hat{a}_{dij}}{2}\,\Xi^b_{ij}(\eta_i(t)),$$

which shows that each memristive weight consists of a constant nominal part and a state-dependent deviation term. We define

$$A_0 = ((\check{a}_{ij})_{n\times n} + (\hat{a}_{ij})_{n\times n})/2,\ A_{d0} = ((\check{a}_{dij})_{n\times n} + (\hat{a}_{dij})_{n\times n})/2,$$

and

$$\mu^a_{ij} = \sqrt{\frac{|\check{a}_{ij} - \hat{a}_{ij}|}{2}},\ \mu^b_{ij} = \sqrt{\frac{|\check{a}_{dij} - \hat{a}_{dij}|}{2}}.$$

Based on these definitions, the factor matrices can be constructed as

$$\begin{aligned}
A_1 &= (\mu^a_{11}e_1, \ldots, \mu^a_{1n}e_1, \ldots, \mu^a_{n1}e_n, \ldots, \mu^a_{nn}e_n)_{n\times n^2},\\
A_{d1} &= (\mu^b_{11}e_1, \ldots, \mu^b_{1n}e_1, \ldots, \mu^b_{n1}e_n, \ldots, \mu^b_{nn}e_n)_{n\times n^2},\\
A_2 &= (\mu^a_{11}e_1, \ldots, \mu^a_{1n}e_n, \ldots, \mu^a_{n1}e_1, \ldots, \mu^a_{nn}e_n)^T_{n\times n^2},\\
A_{d2} &= (\mu^b_{11}e_1, \ldots, \mu^b_{1n}e_n, \ldots, \mu^b_{n1}e_1, \ldots, \mu^b_{nn}e_n)^T_{n\times n^2},\\
\Xi^a(\eta(t)) &= \mathrm{diag}\{\Xi^a_{11}(\eta_1(t)), \ldots, \Xi^a_{1n}(\eta_1(t)), \ldots, \Xi^a_{n1}(\eta_n(t)), \ldots, \Xi^a_{nn}(\eta_n(t))\},\\
\Xi^b(\eta(t)) &= \mathrm{diag}\{\Xi^b_{11}(\eta_1(t)), \ldots, \Xi^b_{1n}(\eta_1(t)), \ldots, \Xi^b_{n1}(\eta_n(t)), \ldots, \Xi^b_{nn}(\eta_n(t))\},
\end{aligned}$$

where e_i denotes the column vector whose i-th entry is one and all the others are zero. The uncertainty matrices are introduced as

$$\Delta(\eta(t)) \in \mathrm{co}[\Xi^a(\eta(t))],\ \Delta(\eta(t-\rho(t))) \in \mathrm{co}[\Xi^b(\eta(t-\rho(t)))],$$

where co$[\cdot]$ denotes the convex hull. Since each diagonal entry of $\Xi^a(\eta(t))$ and $\Xi^b(\eta(t))$ belongs to $\{-1, 1\}$, it follows that

$$\Delta^T(\eta(t))\Delta(\eta(t)) \le I,\ \Delta^T(\eta(t-\rho(t)))\Delta(\eta(t-\rho(t))) \le I.$$

Therefore, the memristive matrices can be represented in the compact uncertain forms as

$$A(\eta(t)) = A_0 + A_1\Delta(\eta(t))A_2,\ A_d(\eta(t-\rho(t))) = A_{d0} + A_{d1}\Delta(\eta(t-\rho(t)))A_{d2}.$$

Accordingly, similar to [39,47,48], the MBNN in (2.1) can be transformed into the following equivalent uncertain system:

$$\begin{aligned}
\dot{\eta}(t) =& -(D - B(F_0 + F_1\lambda)KC)\eta(t) + (A_0 + A_1\Delta(\eta(t))A_2)\varsigma(\eta(t))\\
&+ (A_{d0} + A_{d1}\Delta(\eta(t-\rho(t)))A_{d2})\varsigma(\eta(t-\rho(t))) + Ew(t).
\end{aligned} \tag{2.3}$$

2.3. Performance definitions, an assumption, and lemmas

Definition 1. *System (2.3) is said to possess $\mathcal{H}_\infty$ disturbance-attenuation level $\gamma_1 > 0$, if, under zero initial states,*

$$\int_0^\infty y^T(r)y(r)dr \le \gamma_1^2 \int_0^\infty w^T(r)w(r)dr \tag{2.4}$$

holds for any $w(t) \in L_2[0,\infty)$.

Definition 2. *System (2.3) is said to possess $\mathcal{L}_2 - \mathcal{L}_\infty$ disturbance-attenuation level $\gamma_2 > 0$, if, under zero initial states,*

$$\sup_{t\ge 0}\{y^T(t)y(t)\} \le \gamma_2^2 \int_0^\infty w^T(r)w(r)dr \tag{2.5}$$

holds for any $w(t) \in L_2[0,\infty)$.

Assumption 1. *There exists a positive definite diagonal matrix $\Psi = diag\{\Psi_1,\dots,\Psi_n\}$ such that for any $h, v \in \mathbb{R}$ and $k \in \{1,\dots,n\}$,*

$$|\varsigma_k(h) - \varsigma_k(v)| \le \Psi_k|h - v|. \tag{2.6}$$

Remark 1. *Assumption 1 presents a standard Lipschitz-type condition commonly utilized in the studies of recurrent neural networks [49–53]. It is satisfied by various typical activation functions, including the hyperbolic tangent, sigmoid, and piecewise linear saturating functions.*

Lemma 1. *[54] (BLI) Given a matrix $W \in \mathbb{S}_n^+$ and a differentiable function $\eta : [l,u] \to \mathbb{R}^n$,*

$$\int_l^u \dot\eta^T(r)W\dot\eta(r)\,dr \ge \frac{1}{u-l}\bar\eta^T diag\{W, 3W, 5W\}\,\bar\eta$$

holds, where

$$\bar\eta = \begin{bmatrix} \eta(u) - \eta(l) \\ \eta(u) + \eta(l) - \dfrac{2}{u-l}\int_l^u \eta(r)dr \\ \eta(u) - \eta(l) - \dfrac{6}{u-l}\int_l^u \beta_{l,u}(r)\eta(r)dr \end{bmatrix},\ \beta_{l,u}(r) = 2\left(\frac{r-l}{u-l}\right) - 1.$$

Lemma 2. *[55] (GRCCI) We begin with a matrix $O(\varpi) \in \mathbb{S}^m$ parameterized by ϖ, such that the convex inequality*

$$O(\varpi) \le (1-\varpi)O(0) + \varpi O(1)$$

is valid for any ϖ in $[0,1]$. Suppose there exist a matrix $\tilde W$ in $\mathbb{S}_+^n$ and two matrices Z_1, Z_2 in $\mathbb{R}^{m\times n}$ rendering

$$\begin{bmatrix} O(\varpi) - \Gamma^T\mathcal{W}(\varpi)\Gamma - \mathrm{He}\left(\Gamma^T\begin{bmatrix}(1-\varpi)Z_1^T \\ \varpi Z_2^T\end{bmatrix}\right) & * \\ \varpi Z_1^T + (1-\varpi)Z_2^T & -\tilde W \end{bmatrix} < 0$$

for $\varpi = \{0,1\}$, where

$$\mathcal{W}(\varpi) = \begin{bmatrix}(2-\varpi)\tilde W & 0 \\ 0 & (1+\varpi)\tilde W\end{bmatrix}.$$

Then,

$$O(\varpi) - \zeta(\varpi) < 0, \forall \varpi \in (0,1),$$

holds, where

$$\zeta(\varpi) = \Gamma^T \begin{bmatrix} \dfrac{1}{\varpi}\tilde{W} & 0 \\ 0 & \dfrac{1}{1-\varpi}\tilde{W} \end{bmatrix} \Gamma.$$

Lemma 3. *[56] For any vectors $h, v \in \mathbb{R}^n$, a scalar $q > 0$, and a positive definite matrix $S \in \mathbb{R}^{n\times n}$, the following inequality holds:*

$$2h^T v \le \frac{1}{q} h^T S h + q v^T S^{-1} v.$$

Lemma 4. *[57] (Schur's complement) Let $\bar{\eta} \in \mathbb{S}^n$ be partitioned as $\bar{\eta} = \begin{bmatrix} R_{11} & R_{12} \\ * & R_{22} \end{bmatrix}$, and then $\bar{\eta} < 0$ holds if and only if*

$$R_{22} < 0,\ R_{11} - R_{12}R_{22}^{-1}R_{12}^T < 0.$$

Lemma 5. *[58] Let $m \in \mathbb{N}$. If there exist positive scalars ϑ_i and matrices Ω, P_i, Q_i, R_i $(i = 1, \ldots, m)$ such that*

$$\begin{bmatrix} \Omega & P_1 + \vartheta Q_1 \ \cdots \ P_m + \vartheta_m Q_m \\ * & \mathrm{diag}\{-\vartheta_1 R_1 - \vartheta_1 R_1^T, \ \cdots, \ -\vartheta_m R_m - \vartheta_m R_m^T\} \end{bmatrix} < 0,$$

then the following inequality holds:

$$\Omega + \sum_{i=1}^{m} \mathrm{He}\Big(P_i R_i^{-1} Q_i^T\Big) < 0.$$

Now, the problem under consideration can be formulated as follows: For the MBNN in (2.1) with time-varying delays, we design a fault-resilient output-feedback controller to simultaneously guarantee the $\mathcal{H}_\infty$ and $\mathcal{L}_2 - \mathcal{L}_\infty$ disturbance attenuation of the resulting closed loop of the MBNN in (2.3), as defined in Definitions 1 and 2, respectively.

3. $\mathcal{H}_\infty$ and $\mathcal{L}_2 - \mathcal{L}_\infty$ performance analysis

To improve readability, several augmented vectors and selector matrices are introduced to represent the current state, delayed states, and related integral terms in a unified form. Specifically, the selector matrices κ_i extract the corresponding components, while the vectors $\delta_0(t)$–$\delta_6(t)$ characterize the delay-related state information and integral terms. The overall vector $\hat{\delta}(t)$ then collects all variables needed in the subsequent analysis. The following notations are adopted:

$$\begin{aligned}
\kappa_i &= [0_{n\times(i-1)n}\ I_n\ 0_{n\times(18-i)n}],\ i = 1, \ldots, 18,\\
\varpi &= \frac{\rho(t) - \rho_1}{\rho_{12}},\ 1 - \varpi = \frac{\rho_2 - \rho(t)}{\rho_{12}},\ \rho_{12} = \rho_2 - \rho_1,\\
\overline{\kappa}_0 &= [\kappa_{15}^T \kappa_1^T - \kappa_2^T \kappa_1^T + \kappa_2^T - 2\kappa_5^T \kappa_2^T - \kappa_4^T \hat{\overline{\kappa}}_0^T]^T,\\
\hat{\overline{\kappa}}_0 &= \rho_{12}(\kappa_2 + \kappa_4) - 2(\kappa_{11} + \kappa_{13}),\\
\overline{\kappa}_1(\varpi) &= [\kappa_1^T \rho_1 \kappa_5^T \rho_1 \kappa_6^T \kappa_{11}^T + \kappa_{13}^T \hat{\overline{\kappa}}_1^T(\varpi)]^T,\\
\hat{\overline{\kappa}}_1(\varpi) &= (1 - \varpi)\rho_{12}(\kappa_{11} + \kappa_{14}) + \varpi\rho_{12}(\kappa_{12} - \kappa_{13}),
\end{aligned}$$

$$
\begin{aligned}
\overline{\kappa}_2 &= [\kappa_1^T - \kappa_2^T \ \kappa_1^T + \kappa_2^T - 2\kappa_5^T \ \kappa_1^T - \kappa_2^T - 6\kappa_6^T]^T,\\
\overline{\kappa}_3 &= [\kappa_2^T - \kappa_3^T \ \kappa_2^T + \kappa_3^T - 2\kappa_7^T \ \kappa_2^T - \kappa_3^T - 6\kappa_8^T]^T,\\
\overline{\kappa}_4 &= [\kappa_3^T - \kappa_4^T \ \kappa_3^T + \kappa_4^T - 2\kappa_9^T \ \kappa_3^T - \kappa_4^T - 6\kappa_{10}^T]^T,\\
\Gamma &= [\overline{\kappa}_3^T \ \overline{\kappa}_4^T]^T, \ \eta_t(r) = \eta(t+r),\\
\overline{\rho}_{1,\kappa}(\varpi) &= \varpi\rho_{12}[\kappa_7^T \ \kappa_8^T]^T - [\kappa_{11}^T \ \kappa_{12}^T]^T,\\
\overline{\rho}_{2,\kappa}(\varpi) &= (1-\varpi)\rho_{12}[\kappa_9^T \ \kappa_{10}^T]^T - [\kappa_{13}^T \ \kappa_{14}^T]^T,\\
\delta_0(t) &= [\eta^T(t) \ \eta^T(t-\rho_1) \ \eta^T(t-\rho(t)) \ \eta^T(t-\rho_2)]^T,\\
\delta_1(t) &= \frac{1}{\rho_1}\left[\int_{-\rho_1}^{0} \eta_t^T(r)dr \ \int_{-\rho_1}^{0} \beta_1(r)\eta_t^T(r)dr\right]^T,\\
\delta_2(t) &= \frac{1}{\rho(t)-\rho_1}\left[\int_{-\rho(t)}^{-\rho_1} \eta_t^T(r)dr \ \int_{-\rho(t)}^{-\rho_1} \beta_2(r)\eta_t^T(r)dr\right]^T,\\
\delta_3(t) &= \frac{1}{\rho_2-\rho(t)}\left[\int_{-\rho_2}^{-\rho(t)} \eta_t^T(r)dr \ \int_{-\rho_2}^{-\rho(t)} \beta_3(r)\eta_t^T(r)dr\right]^T,\\
\delta_4(t) &= \left[\int_{-\rho(t)}^{-\rho_1} \eta_t^T(r)dr \ \int_{-\rho(t)}^{-\rho_1} \beta_2(r)\eta_t^T(r)dr\right]^T,\\
\delta_5(t) &= \left[\int_{-\rho_2}^{-\rho(t)} \eta_t^T(r)dr \ \int_{-\rho_2}^{-\rho(t)} \beta_3(r)\eta_t^T(r)dr\right]^T,\\
\delta_6(t) &= \left[\int_{-\rho_2}^{-\rho_1} \eta_t^T(r)dr\,\rho_{12} \int_{-\rho_2}^{-\rho_1} \beta_4(r)\eta_t^T(r)dr\right]^T,\\
\hat{\delta}(t) &= [\delta_0^T(t) \ \dots \ \delta_5^T(t) \ \dot{\eta}^T(t) \ \varsigma^T(\eta(t)) \ \varsigma^T(\eta(t-\rho(t))) \ w^T(t)]^T,
\end{aligned}
$$

where

$$
\begin{aligned}
&\beta_1(r) = 2\frac{r+\rho_1}{\rho_1} - 1, \quad \beta_2(r) = 2\frac{r+\rho(t)}{\rho(t)-\rho_1} - 1,\\
&\beta_3(r) = 2\frac{r+\rho_2}{\rho_2-\rho(t)} - 1, \quad \beta_4(r) = 2\frac{r+\rho_2}{\rho_{12}} - 1.
\end{aligned}
$$

Using the aforementioned notations, we now present the analysis condition for the MBNN in (2.3).

Theorem 1. *The MBNN in (2.3) possesses $\mathcal{H}_\infty$ and $\mathcal{L}_2 - \mathcal{L}_\infty$ disturbance-attenuation levels $\gamma_1 > 0$ and $\gamma_2 > 0$, respectively, if, for prescribed delay bounds $\rho_1 > 0$ and $\rho_2 > 0$, there exist matrices $L_1, L_2 \in \mathbb{R}^{n\times n}$, $M_1, M_2 \in \mathbb{R}^{18n\times 2n}$, $\Pi = (\Pi_{jk})_{5\times 5} \in \mathbb{S}_+^{5n}$, $N_1, N_2, W_1, W_2 \in \mathbb{S}_+^n$, positive diagonal matrices $Q_1, Q_2, \Theta_1, \Theta_2, \Theta_3, \Theta_4$, and matrices $Z_1, Z_2 \in \mathbb{R}^{18n\times 3n}$ satisfying*

$$
\begin{bmatrix}
O_0^i(\varpi, Z) & \varpi Z_1 + (1-\varpi)Z_2 & \Phi_1 & \Phi_2 & \Phi_3 & \Phi_4\\
* & -\tilde{W}_2 & 0 & 0 & 0 & 0\\
* & * & -\Theta_1 & 0 & 0 & 0\\
* & * & * & -\Theta_3 & 0 & 0\\
* & * & * & * & -\Theta_2 & 0\\
* & * & * & * & * & -\Theta_4
\end{bmatrix} < 0, \tag{3.1}
$$

$$
\gamma_2^2\Pi_{11} - \gamma_1^2 C^T C \geq 0 \tag{3.2}
$$

for any $\varpi \in \{0, 1\}$*, where*

$$
\begin{aligned}
O_0^i(\varpi, Z) &= O_0^i(\varpi) + \kappa_1^T C^T C \kappa_1 + (1-\gamma_1^2)\kappa_{18}^T I \kappa_{18} - \Gamma^T \mathcal{W}_2(\varpi)\Gamma - \mathrm{He}\left(\Gamma^T \begin{bmatrix} (1-\varpi)Z_1^T \\ \varpi Z_2^T \end{bmatrix}\right), \\
O_0^i(\varpi) &= He\left[(\bar{\kappa}_1^T(\varpi)\Pi\bar{\kappa}_0) + M_1\bar{\rho}_{1,\kappa}(\varpi) + M_2\bar{\rho}_{2,\kappa}(\varpi)\right] + \hat{N} - \bar{\kappa}_2^T\tilde{W}_1\bar{\kappa}_2 + \hat{U} \\
&\quad + 2\kappa_1^T(-L_1^T - D_K^T L_2)\kappa_{15} + 2\kappa_1^T(L_1^T A_0 + Q_1\Psi)\kappa_{16} \\
&\quad + 2\kappa_{15}^T L_2^T A_0 \kappa_{16} + 2\kappa_1^T L_1^T A_{d0}\kappa_{17} + 2\kappa_{15}^T L_2^T A_{d0}\kappa_{17} + 2\kappa_3^T Q_2 \Psi \kappa_{17} \\
&\quad + 2\kappa_1^T L_1^T E\kappa_{18} + 2\kappa_{15}^T L_2^T E\kappa_{18} - \kappa_{18}^T\kappa_{18}, \\
\hat{N} &= diag\left\{N_1,\ -N_1 + N_2,\ 0_{n\times n},\ -N_2,\ 0_{14n\times 14n}\right\}, \\
\hat{U} &= diag\{He(-L_1^T D_K),\ 0_{13n\times 13n},\ He(-L_2^T) + \rho_1^2 W_1 + \rho_{12}^2 W_2, \\
&\quad He(-Q_1) + A_2^T(\Theta_1 + \Theta_2)A_2,\ He(-Q_2) + A_{d2}^T(\Theta_3 + \Theta_4)A_{d2},\ 0_{n\times n}\}, \\
\tilde{W}_i &= diag\{W_i,\ 3W_i,\ 5W_i\}, \\
\mathcal{W}_i(\varpi) &= \begin{bmatrix} (2-\varpi)\tilde{W}_i & 0 \\ 0 & (1+\varpi)\tilde{W}_i \end{bmatrix}, \\
D_K &= D - B(F_0 + F_1\lambda)KC, \\
\Phi_1 &= \begin{bmatrix} A_1^T L_1 & 0_{2n\times 17n} \end{bmatrix}^T, \\
\Phi_2 &= \begin{bmatrix} A_{d1}^T L_1 & 0_{2n\times 17n} \end{bmatrix}^T, \\
\Phi_3 &= \begin{bmatrix} 0_{2n\times 14n} & A_1^T L_2 & 0_{2n\times 3n} \end{bmatrix}^T, \\
\Phi_4 &= \begin{bmatrix} 0_{2n\times 14n} & A_{d1}^T L_2 & 0_{2n\times 3n} \end{bmatrix}^T.
\end{aligned}
$$

Proof. With the notations defined above, we have

$$
\eta(t) = \kappa_1\hat{\delta}(t),\ \rho_1\delta_1(t) = \begin{bmatrix} \rho_1\kappa_5 \\ \rho_1\kappa_6 \end{bmatrix}\hat{\delta}(t).
$$

From $\delta_6(t)$, the first n components are given by

$$
\begin{aligned}
\int_{-\rho_2}^{-\rho_1} \eta_t(r)dr &= \int_{-\rho(t)}^{-\rho_1} \eta_t(r)dr + \int_{-\rho_2}^{-\rho(t)} \eta_t(r)dr \\
&= \kappa_{11}\hat{\delta}(t) + \kappa_{13}\hat{\delta}(t) = (\kappa_{11} + \kappa_{13})\hat{\delta}(t).
\end{aligned}
$$

For the other n components, $\beta_4(r)$ admits two equivalent representations, each obtained from $\beta_2(r)$ and $\beta_3(r)$ in turn. Specifically, we have

$$
\begin{aligned}
\rho_{12}\beta_4(r) &= \rho_{12}(2\frac{r+\rho_2}{\rho_{12}} - 1) = 2(r+\rho_2) - (\rho_2 - \rho_1) = 2r + \rho_2 + \rho_1 \\
&= 2r + 2\rho(t) - 2\rho(t) + \rho_2 + \rho_1 = 2(r+\rho(t)) - (\rho(t) - \rho_1) - (\rho(t) - \rho_2) \\
&= (\rho(t) - \rho_1)(2\frac{r+\rho(t)}{\rho(t) - \rho_1} - 1) + (\rho_2 - \rho(t)) \\
&= (\rho(t) - \rho_1)\beta_2(r) - (\rho_2 - \rho(t))
\end{aligned}
$$

$$= 2r + 2\rho_2 - (\rho_2 - \rho(t)) - (\rho(t) - \rho_1) = 2(r + \rho_2) - (\rho_2 - \rho(t)) - (\rho(t) - \rho_1)$$
$$= (\rho_2 - \rho(t))(2\frac{r + \rho_2}{\rho_2 - \rho(t)} - 1) - (\rho(t) - \rho_1)$$
$$= (\rho_2 - \rho(t))\beta_3(r) - (\rho(t) - \rho_1). \tag{3.3}$$

Substituting (3.3) into the remaining n components yields

$$\rho_{12}\int_{-\rho_2}^{-\rho_1}\beta_4(r)\eta_t(r)dr = \rho_{12}\left(\int_{-\rho(t)}^{-\rho_1}\beta_4(r)\eta_t(r)dr + \int_{-\rho_2}^{-\rho(t)}\beta_4(r)\eta_t(r)dr\right)$$
$$= \rho_{12}\beta_4(r)\int_{-\rho(t)}^{-\rho_1}\eta_t(r)dr + \rho_{12}\beta_4(r)\int_{-\rho_2}^{-\rho(t)}\eta_t(r)dr$$
$$= [(\rho(t) - \rho_1)\beta_2(r) + (\rho_2 - \rho(t))]\int_{-\rho(t)}^{-\rho_1}\eta_t(r)dr + [(\rho_2 - \rho(t))\beta_3(r) - (\rho(t) - \rho_1)]\int_{-\rho_2}^{-\rho(t)}\eta_t(r)dr$$
$$= (\rho_2 - \rho(t))\left[\int_{-\rho(t)}^{-\rho_1}\eta_t(r)dr + \beta_3(r)\int_{-\rho_2}^{-\rho(t)}\eta_t(r)dr\right]$$
$$+ (\rho(t) - \rho_1)\left[\beta_2(r)\int_{-\rho(t)}^{-\rho_1}\eta_t(r)dr - \int_{-\rho_2}^{-\rho(t)}\eta_t(r)dr\right]$$
$$= (\rho_2 - \rho(t))(\kappa_{11} + \kappa_{14}) + (\rho(t) - \rho_1)(\kappa_{12} - \kappa_{13}) = (1 - \varpi)\rho_{12}(\kappa_{11} + \kappa_{14}) + \varpi\rho_{12}(\kappa_{12} - \kappa_{13})$$
$$= \hat{\overline{\kappa}}_1(\varpi).$$

Accordingly, we obtain

$$\tilde{\eta}(t) = \begin{bmatrix}\eta(t)\\ \rho_1\delta_1(t)\\ \delta_6(t)\end{bmatrix} = \begin{bmatrix}\kappa_1\\ \rho_1\kappa_5\\ \rho_1\kappa_6\\ \kappa_{11} + \kappa_{13}\\ \hat{\overline{\kappa}}_1(\varpi)\end{bmatrix}\hat{\delta}(t) = \overline{\kappa}_1(\varpi)\hat{\delta}(t). \tag{3.4}$$

Given the notations introduced earlier, we can also deduce that

$$\rho_1\dot{\delta}_1(t) = \begin{bmatrix}\eta(t) - \eta(t - \rho_1)\\ \eta(t) + \eta(t - \rho_1) - \frac{2}{\rho_1}\int_{-\rho_1}^{0}\eta_t(r)dr\end{bmatrix} = \begin{bmatrix}\kappa_1 - \kappa_2\\ \kappa_1 + \kappa_2 - 2\kappa_5\end{bmatrix}\hat{\delta}(t),$$
$$\dot{\delta}_6(t) = \begin{bmatrix}\eta(t - \rho_1) - \eta(t - \rho_2)\\ \rho_{12}(\eta(t - \rho_1) + \eta(t - \rho_2)) - 2(\int_{-\rho(t)}^{-\rho_1}\eta_t(r)dr + \int_{-\rho_2}^{-\rho(t)}\eta_t(r)dr)\end{bmatrix}$$
$$= \begin{bmatrix}\kappa_2 - \kappa_4\\ \rho_{12}(\kappa_2 + \kappa_4) - 2(\kappa_{11} + \kappa_{13})\end{bmatrix}\hat{\delta}(t) = \begin{bmatrix}\kappa_2 - \kappa_4\\ \hat{\overline{\kappa}}_0\end{bmatrix}\hat{\delta}(t),$$

which further implies

$$\dot{\tilde{\eta}}(t) = \begin{bmatrix}\dot{\eta}(t)\\ \rho_1\dot{\delta}_1(t)\\ \dot{\delta}_6(t)\end{bmatrix} = \begin{bmatrix}\kappa_{15}\\ \kappa_1 - \kappa_2\\ \kappa_1 + \kappa_2 - 2\kappa_5\\ \kappa_2 - \kappa_4\\ \hat{\overline{\kappa}}_0\end{bmatrix}\hat{\delta}(t) = \overline{\kappa}_0\hat{\delta}(t). \tag{3.5}$$

In addition, by applying the defined structure of $\hat{\delta}(t)$, it becomes evident that

$$\begin{aligned}\overline{\rho}_{1,\kappa}(\varpi)\hat{\delta}(t) &= (\varpi\rho_{12}\begin{bmatrix}\kappa_7\\ \kappa_8\end{bmatrix} - \begin{bmatrix}\kappa_{11}\\ \kappa_{12}\end{bmatrix})\hat{\delta}(t) = ((\rho(t)-\rho_1)\begin{bmatrix}\kappa_7\\ \kappa_8\end{bmatrix} - \begin{bmatrix}\kappa_{11}\\ \kappa_{12}\end{bmatrix})\hat{\delta}(t)\\ &= (\rho(t)-\rho_1)\delta_2(t) - \delta_4(t) = 0,\\ \overline{\rho}_{2,\kappa}(\varpi)\hat{\delta}(t) &= ((1-\varpi)\rho_{12}\begin{bmatrix}\kappa_9\\ \kappa_{10}\end{bmatrix} - \begin{bmatrix}\kappa_{13}\\ \kappa_{14}\end{bmatrix})\hat{\delta}(t) = ((\rho_2-\rho(t))\begin{bmatrix}\kappa_9\\ \kappa_{10}\end{bmatrix} - \begin{bmatrix}\kappa_{13}\\ \kappa_{14}\end{bmatrix})\hat{\delta}(t)\\ &= (\rho_2-\rho(t))\delta_3(t) - \delta_5(t) = 0.\end{aligned}$$

With the aid of the matrices $\overline{\rho}_{1,\kappa}(\varpi)$ and $\overline{\rho}_{2,\kappa}(\varpi)$ introduced above, one can obtain the following equality for arbitrary matrices $M_1, M_2 \in \mathbb{R}^{18n\times 2n}$:

$$2\hat{\delta}^T(t)(M_1\overline{\rho}_{1,\kappa}(\varpi) + M_2\overline{\rho}_{2,\kappa}(\varpi))\hat{\delta}(t) = 0. \tag{3.6}$$

Subsequently, by introducing the free-weighting matrices $L_1, L_2 \in \mathbb{R}^{n\times n}$ as in [59], the dynamics of the MBNN in (2.3) guarantee the satisfaction of the following relation:

$$\begin{aligned}0 &= 2[\eta^T(t)L_1^T + \dot{\eta}^T(t)L_2^T]\Big[-\dot{\eta}(t) - D_K\eta(t) + A_0\varsigma(\eta(t)) + A_{d0}\varsigma(\eta(t-\rho(t)))\Big]\\ &\quad + 2[\eta^T(t)L_1^T + \dot{\eta}^T(t)L_2^T]\Big[A_1\Delta(\eta(t))A_2\varsigma(\eta(t)) + A_{d1}\Delta(\eta(t-\rho(t)))A_{d2}\varsigma(\eta(t-\rho(t))) + Ew(t)\Big].\end{aligned} \tag{3.7}$$

Noting that the uncertainty matrices satisfy $\Delta(\eta(t))\Delta(\eta(t)) \le I$ and $\Delta(\eta(t-\rho(t)))\Delta(\eta(t-\rho(t))) \le I$, and introducing positive diagonal matrices Θ_1, Θ_2, Θ_3, and Θ_4, the following inequalities can be derived by applying Lemma 3:

$$2\eta^T(t)L_1^TA_1\Delta(\eta(t))A_2\varsigma(\eta(t)) \le \eta^T(t)L_1^TA_1\Theta_1^{-1}A_1^TL_1\eta(t) + \varsigma^T(\eta(t))A_2^T\Theta_1A_2\varsigma(\eta(t)), \tag{3.8}$$

$$2\dot{\eta}^T(t)L_2^TA_1\Delta(\eta(t))A_2\varsigma(\eta(t)) \le \dot{\eta}^T(t)L_2^TA_1\Theta_2^{-1}A_1^TL_2\dot{\eta}(t) + \varsigma^T(\eta(t))A_2^T\Theta_2A_2\varsigma(\eta(t)), \tag{3.9}$$

$$\begin{aligned}&2\eta^T(t)L_1^TA_{d1}\Delta(\eta(t-\rho(t)))A_{d2}\varsigma(\eta(t-\rho(t)))\\ &\quad\le \eta^T(t)L_1^TA_{d1}\Theta_3^{-1}A_{d1}^TL_1\eta(t) + \varsigma^T(\eta(t-\rho(t)))A_{d2}^T\Theta_3A_{d2}\varsigma(\eta(t-\rho(t))),\end{aligned} \tag{3.10}$$

$$\begin{aligned}&2\dot{\eta}^T(t)L_2^TA_{d1}\Delta(\eta(t-\rho(t)))A_{d2}\varsigma(\eta(t-\rho(t)))\\ &\quad\le \dot{\eta}^T(t)L_2^TA_{d1}\Theta_4^{-1}A_{d1}^TL_2\dot{\eta}(t) + \varsigma^T(\eta(t-\rho(t)))A_{d2}^T\Theta_4A_{d2}\varsigma(\eta(t-\rho(t))).\end{aligned} \tag{3.11}$$

Utilizing the Lipschitz condition for the neuron activation functions given in (2.6), the subsequent inequalities are obtained:

$$0 \le 2\eta^T(t)Q_1\Psi\varsigma(\eta(t)) - 2\varsigma^T(\eta(t))Q_1\varsigma(\eta(t)), \tag{3.12}$$

$$0 \le 2\eta^T(t-\rho(t))Q_2\Psi\varsigma(\eta(t-\rho(t))) - 2\varsigma^T(\eta(t-\rho(t)))Q_2\varsigma(\eta(t-\rho(t))). \tag{3.13}$$

To analyze the dual performance of the MBNN in (2.3), we construct the following LKF:

$$\begin{aligned}V(t) &= V_1(\eta_t) + V_2(\eta_t) + V_3(\eta_t,\dot{\eta}_t),\\ V_1(\eta_t) &= \tilde{\eta}^T(t)\Pi\tilde{\eta}(t),\\ V_2(\eta_t) &= \int_{t-\rho_1}^{t}\eta^T(r)N_1\eta(r)dr + \int_{t-\rho_2}^{t-\rho_1}\eta^T(r)N_2\eta(r)dr,\\ V_3(\eta_t,\dot{\eta}_t) &= \rho_1\int_{-\rho_1}^{0}\int_{t+s}^{t}\dot{\eta}^T(r)W_1\dot{\eta}(r)drds + \rho_{12}\int_{-\rho_2}^{-\rho_1}\int_{t+s}^{t}\dot{\eta}^T(r)W_2\dot{\eta}(r)drds,\end{aligned}$$

where

$$\tilde{\eta}(t) = \begin{bmatrix} \eta^T(t) & \rho_1\delta_1^T(t) & \delta_6^T(t) \end{bmatrix}^T.$$

Utilizing (3.4)–(3.6), the derivatives of $V_1(\eta_t)$, $V_2(\eta_t)$, and $V_3(\eta_t)$ can be computed as follows:

$$\begin{aligned}
\dot{V}_1(\eta_t) &= 2\tilde{\eta}^T(t)\Pi\dot{\tilde{\eta}}(t) = 2\hat{\delta}^T(t)\overline{\kappa}_1^T(\varpi)\Pi\overline{\kappa}_0\dot{\hat{\delta}}(t) = \hat{\delta}^T(t)He(\overline{\kappa}_1^T(\varpi)\Pi\overline{\kappa}_0)\dot{\hat{\delta}}(t) \\
&= \hat{\delta}^T(t)He\left[(\overline{\kappa}_1^T(\varpi)\Pi\overline{\kappa}_0) + M_1\overline{\rho}_{1,\kappa}(\varpi) + M_2\overline{\rho}_{2,\kappa}(\varpi)\right]\dot{\hat{\delta}}(t), \qquad (3.14) \\
\dot{V}_2(\eta_t) &= \eta^T(t)N_1\eta(t) - \eta^T(t-\rho_1)N_1\eta(t-\rho_1) + \eta^T(t-\rho_1)N_2\eta(t-\rho_1) - \eta^T(t-\rho_2)N_2\eta(t-\rho_2) \\
&= \hat{\delta}^T(t)\hat{N}\dot{\hat{\delta}}(t), \\
\dot{V}_3(\eta_t,\dot{\eta}_t) &= \rho_1\Big[\int_{-\rho_1}^{0}(\dot{\eta}^T(t)W_1\dot{\eta}(t) - \dot{\eta}^T(t+s)W_1\dot{\eta}(t+s))ds\Big] \\
&\quad + \rho_{12}\Big[\int_{-\rho_2}^{-\rho_1}\dot{\eta}^T(t)W_2\dot{\eta}(t) - \dot{\eta}^T(t+s)W_2\dot{\eta}(t+s)ds\Big] \\
&= \rho_1^2\dot{\eta}^T(t)W_1\dot{\eta}(t) - \rho_1\int_{-\rho_1}^{0}\dot{\eta}^T(t+s)W_1\dot{\eta}(t+s)ds \\
&\quad + \rho_{12}^2\dot{\eta}^T(t)W_2\dot{\eta}(t) - \rho_{12}\int_{-\rho_2}^{-\rho_1}\dot{\eta}^T(t+s)W_2\dot{\eta}(t+s)ds \\
&= \dot{\eta}^T(t)\left(\rho_1^2W_1 + \rho_{12}^2W_2\right)\dot{\eta}(t) - \rho_1\int_{t-\rho_1}^{t}\dot{\eta}^T(r)W_1\dot{\eta}(r)dr - \rho_{12}\int_{t-\rho_2}^{t-\rho_1}\dot{\eta}^T(r)W_2\dot{\eta}(r)dr. \qquad (3.15)
\end{aligned}$$

Then, by combining the system dynamics in (3.7) with the uncertainty bounds in (3.8)–(3.13), an upper bound of $\dot{V}_2(\eta_t)$ is obtained as

$$\begin{aligned}
\dot{V}_2(\eta_t) \le \hat{\delta}^T(t)\Big(&\hat{N} + \hat{U} + 2\kappa_1^T(-L_1^T - D_K^TL_2)\kappa_{15} + 2\kappa_1^T(L_1^TA_0 + Q_1\Psi)\kappa_{16} + 2\kappa_{15}^TL_2^TA_0\kappa_{16} \\
&+ 2\kappa_1^TL_1^TA_{d0}\kappa_{17} + 2\kappa_{15}^TL_2^TA_{d0}\kappa_{17} + 2\kappa_3^TQ_2\Psi\kappa_{17} + 2\kappa_1^TL_1^TE\kappa_{18} + 2\kappa_{15}^TL_2^TE\kappa_{18} \\
&+ \Phi_1\Theta_1^{-1}\Phi_1^T + \Phi_2\Theta_3^{-1}\Phi_2^T + \Phi_3\Theta_2^{-1}\Phi_3^T + \Phi_4\Theta_4^{-1}\Phi_4^T\Big)\hat{\delta}(t). \qquad (3.16)
\end{aligned}$$

Drawing upon Lemmas 1 and 2, we arrive at

$$\begin{aligned}
&-\rho_1\int_{t-\rho_1}^{t}\dot{\eta}^T(r)W_1\dot{\eta}(r)dr \\
&\le -\begin{bmatrix} \eta(t)-\eta(t-\rho_1) \\ \eta(t)+\eta(t-\rho_1) - \frac{2}{\rho_1}\int_{t-\rho_1}^{t}\eta(r)dr \\ \eta(t)-\eta(t-\rho_1) - \frac{6}{\rho_1}\int_{t-\rho_1}^{t}\beta_1(r)\eta(r)dr \end{bmatrix}^T \tilde{W}_1 \begin{bmatrix} \eta(t)-\eta(t-\rho_1) \\ \eta(t)+\eta(t-\rho_1) - \frac{2}{\rho_1}\int_{t-\rho_1}^{t}\eta(r)dr \\ \eta(t)-\eta(t-\rho_1) - \frac{6}{\rho_1}\int_{t-\rho_1}^{t}\beta_1(r)\eta(r)dr \end{bmatrix} \\
&= -\hat{\delta}^T(t)\begin{bmatrix} \kappa_1-\kappa_2 \\ \kappa_1+\kappa_2-2\kappa_5 \\ \kappa_1-\kappa_2-2\kappa_6 \end{bmatrix}^T \tilde{W}_1 \begin{bmatrix} \kappa_1-\kappa_2 \\ \kappa_1+\kappa_2-2\kappa_5 \\ \kappa_1-\kappa_2-2\kappa_6 \end{bmatrix}\hat{\delta}(t) \\
&= -\hat{\delta}^T(t)\overline{\kappa}_2^T\tilde{W}_1\overline{\kappa}_2\hat{\delta}(t),
\end{aligned}$$

and

$$-\rho_{12}\int_{t-\rho_2}^{t-\rho_1}\dot{\eta}^T(r)W_2\dot{\eta}(r)dr = -\rho_{12}\int_{t-\rho_2}^{t-\rho(t)}\dot{\eta}^T(r)W_2\dot{\eta}(r)dr - \rho_{12}\int_{t-\rho(t)}^{t-\rho_1}\dot{\eta}^T(r)W_2\dot{\eta}(r)dr$$

$$
\begin{aligned}
&\leq -\frac{\rho_{12}}{\rho_2-\rho(t)}\hat{\delta}^T(t)\begin{bmatrix}\kappa_3-\kappa_4\\ \kappa_3+\kappa_4-2\kappa_9\\ \kappa_3-\kappa_4-6\kappa_{10}\end{bmatrix}^T\tilde{W}_2\begin{bmatrix}\kappa_3-\kappa_4\\ \kappa_3+\kappa_4-2\kappa_9\\ \kappa_3-\kappa_4-6\kappa_{10}\end{bmatrix}\hat{\delta}(t)\\
&-\frac{\rho_{12}}{\rho(t)-\rho_1}\hat{\delta}^T(t)\begin{bmatrix}\kappa_2-\kappa_3\\ \kappa_2+\kappa_3-2\kappa_7\\ \kappa_2-\kappa_3-6\kappa_8\end{bmatrix}^T\tilde{W}_2\begin{bmatrix}\kappa_2-\kappa_3\\ \kappa_2+\kappa_3-2\kappa_7\\ \kappa_2-\kappa_3-6\kappa_8\end{bmatrix}\hat{\delta}(t)\\
&=-\frac{1}{1-\varpi}\hat{\delta}^T(t)\bar{\kappa}_4^T\tilde{W}_2\bar{\kappa}_4\hat{\delta}(t)-\frac{1}{\varpi}\hat{\delta}^T(t)\bar{\kappa}_3^T\tilde{W}_2\bar{\kappa}_3\hat{\delta}(t)\\
&=-\hat{\delta}^T(t)\zeta_2(\varpi)\hat{\delta}(t),
\end{aligned}
$$

where

$$
\zeta_2(\varpi)=\Gamma^T\begin{bmatrix}\frac{1}{\varpi}\tilde{W}_2 & 0\\ 0 & \frac{1}{1-\varpi}\tilde{W}_2\end{bmatrix}\Gamma.
$$

Substituting the above two inequalities into (3.15), the derivative of $V_3(\eta_t,\dot{\eta}_t)$ can be upper-bounded as

$$
\begin{aligned}
\dot{V}_3(\eta_t,\dot{\eta}_t)&\leq\dot{\eta}^T(t)(\rho_1^2W_1+\rho_{12}^2W_2)\dot{\eta}(t)-\hat{\delta}^T(t)\bar{\kappa}_2^T\tilde{W}_1\bar{\kappa}_2\hat{\delta}(t)-\hat{\delta}^T(t)\zeta_2(\varpi)\hat{\delta}(t)\\
&=\hat{\delta}^T(t)(\kappa_{15}^T(\rho_1^2W_1+\rho_{12}^2W_2)\kappa_{15}-\bar{\kappa}_2^T\tilde{W}_1\bar{\kappa}_2-\zeta_2(\varpi))\hat{\delta}(t).
\end{aligned}\tag{3.17}
$$

Since $V(t)=V_1(\eta_t)+V_2(\eta_t)+V_3(\eta_t,\dot{\eta}_t)$, using (3.14), (3.16), and (3.17) yields

$$
\begin{aligned}
\dot{V}(t)\leq\ &\hat{\delta}^T(t)(\mathrm{He}\left[(\bar{\kappa}_1^T(\varpi)\Pi\bar{\kappa}_0)+M_1\bar{\rho}_{1,\kappa}(\varpi)+M_2\bar{\rho}_{2,\kappa}(\varpi)\right]+\hat{N}-\bar{\kappa}_2^T\tilde{W}_1\bar{\kappa}_2-\zeta_2(\varpi)+\hat{U}\\
&+2\kappa_1^T(-L_1^T-D_K^TL_2)\kappa_{15}+2\kappa_1^T(L_1^TA_0+Q_1\Psi)\kappa_{16}\\
&+2\kappa_{15}^TL_2^TA_0\kappa_{16}+2\kappa_1^TL_1^TA_{d0}\kappa_{17}+2\kappa_{15}^TL_2^TA_{d0}\kappa_{17}+2\kappa_3^TQ_2\Psi\kappa_{17}\\
&+2\kappa_1^TL_1^TE\kappa_{18}+2\kappa_{15}^TL_2^TE\kappa_{18}+\Phi_1\Theta_1^{-1}\Phi_1^T+\Phi_2\Theta_3^{-1}\Phi_2^T+\Phi_3\Theta_2^{-1}\Phi_3^T+\Phi_4\Theta_4^{-1}\Phi_4^T)\hat{\delta}(t)\\
=\ &\hat{\delta}^T(t)(O_0^i(\varpi,\Theta)-\zeta_2(\varpi))\hat{\delta}(t)+w^T(t)w(t),
\end{aligned}\tag{3.18}
$$

where

$$
O_0^i(\varpi,\Theta)=O_0^i(\varpi)+\Phi_1\Theta_1^{-1}\Phi_1^T+\Phi_2\Theta_3^{-1}\Phi_2^T+\Phi_3\Theta_2^{-1}\Phi_3^T+\Phi_4\Theta_4^{-1}\Phi_4^T.
$$

To establish the dual performance criterion given zero initial conditions, we formulate the subsequent index function:

$$
\begin{aligned}
J(t)&=\dot{V}(t)+y^T(t)y(t)-\gamma_1^2w^T(t)w(t)\\
&\leq\hat{\delta}^T(t)(O_0^i(\varpi,\Theta)-\zeta_2(\varpi))\hat{\delta}(t)+w^T(t)w(t)+\eta^T(t)C^TC\eta(t)-\gamma_1^2w^T(t)w(t)\\
&=\hat{\delta}^T(t)\left[O_0^i(\varpi,\Theta)+\kappa_1^TC^TC\kappa_1+(1-\gamma_1^2)\kappa_{18}^TI\kappa_{18}-\zeta_2(\varpi)\right]\hat{\delta}(t).
\end{aligned}\tag{3.19}
$$

By virtue of Lemma 4, it follows from (3.1) that

$$
\begin{bmatrix}O_0^i(\varpi,\Theta)+\kappa_1^TC^TC\kappa_1+(1-\gamma_1^2)\kappa_{18}^TI\kappa_{18}-\Gamma^T\mathcal{W}_2(\varpi)\Gamma-\mathrm{He}\left(\Gamma^T\begin{bmatrix}(1-\varpi)Z_1^T\\ \varpi Z_2^T\end{bmatrix}\right) & *\\ \varpi Z_1^T+(1-\varpi)Z_2^T & -\tilde{W}_2\end{bmatrix}<0
$$

holds for any $\varpi \in \{0, 1\}$. In light of Lemma 2, this implies that

$$O_0^i(\varpi, \Theta) + \kappa_1^T C^T C \kappa_1 + (1 - \gamma_1^2)\kappa_{18}^T I \kappa_{18} - \zeta_2(\varpi) < 0$$

for any $\varpi \in [0, 1]$. Consequently, in view of (3.19), we can write

$$\dot{V}(t) \leq -y^T(t)y(t) + \gamma_1^2 w^T(t)w(t). \tag{3.20}$$

Invoking the Newton-Leibniz formula under the premise of zero initial states provides:

$$V(\infty) - V(0) = \int_0^\infty \dot{V}(t)dt \leq -\int_0^\infty y^T(t)y(t)dt + \gamma_1^2 \int_0^\infty w^T(t)w(t)dt. \tag{3.21}$$

By transforming, we can express (3.21) as

$$\int_0^\infty y^T(t)y(t)dt \leq \gamma_1^2 \int_0^\infty w^T(t)w(t)dt - V(\infty).$$

Since $V(\infty) \geq 0$, we obtain (2.4), which implies the desired $\mathcal{H}_\infty$ performance is satisfied by Definition 1. Subsequently, we proceed to analyze the $\mathcal{L}_2 - \mathcal{L}_\infty$ performance of the MBNN. Combining (3.20) and the fact that $y^T(t)y(t) \geq 0$, it holds that

$$\dot{V}(t) \leq \gamma_1^2 w^T(t)w(t). \tag{3.22}$$

Postulating a zero initial condition where $V(0) = 0$, integrating (3.22) from 0 to any $t > 0$ yields

$$V(t) = \int_0^t \dot{V}(r)dr \leq \gamma_1^2 \int_0^t w^T(r)w(r)dr \leq \gamma_1^2 \int_0^\infty w^T(r)w(r)dr. \tag{3.23}$$

From the definition of the LKF, it holds that

$$V(t) \geq \tilde{\eta}^T(t)\Pi\tilde{\eta}(t) \geq \eta^T(t)\Pi_{11}\eta(t). \tag{3.24}$$

Combining (3.23) and (3.24), we obtain that

$$\eta^T(t)\Pi_{11}\eta(t) \leq \gamma_1^2 \int_0^\infty w^T(r)w(r)dr. \tag{3.25}$$

According to (3.2) and the output relation $y(t) = C\eta(t)$, it follows that

$$\gamma_1^2 y^T(t)y(t) \leq \gamma_2^2 \eta^T(t)\Pi_{11}\eta(t). \tag{3.26}$$

Multiplying both sides of (3.25) by γ_2^2 leads to

$$\gamma_2^2 \eta^T(t)\Pi_{11}\eta(t) \leq \gamma_2^2\gamma_1^2 \int_0^\infty w^T(r)w(r)dr. \tag{3.27}$$

By combining (3.26) with (3.27), we have

$$\gamma_1^2 y^T(t)y(t) \leq \gamma_2^2\gamma_1^2 \int_0^\infty w^T(r)w(r)\,dr.$$

Dividing both sides by γ_1^2 and taking the supremum over $t > 0$, we arrive at (2.5), which implies the desired $\mathcal{L}_2 - \mathcal{L}_\infty$ performance is satisfied by Definition 2. The proof of the theorem is hereby complete. □

Remark 2. *The derivation of Theorem 1 follows a unified framework to guarantee both $\mathcal{H}_\infty$ and $\mathcal{L}_2-\mathcal{L}_\infty$ disturbance attenuation for delayed MBNN (2.3). First, auxiliary terms are introduced to reformulate the time-varying delay components into an augmented representation. Then, by incorporating free-weighting matrices, the system dynamics are embedded into the analysis, and an LKF consisting of three components is constructed to capture the state, distributed delay, and derivative information. Finally, by employing the BLI, GRCCI, and Lipschitz condition, a delay-dependent condition ensuring dual disturbance attenuation is derived. Notably, the BLI is more general than the Jensen inequality and the Wirtinger-based integral inequality, while the GRCCI encompasses the classical reciprocally convex combination inequality as a special case [55, 60]. The combined use of the BLI and GRCCI helps reduce approximation errors in bounding the integral terms in (3.18), thereby alleviating conservatism in the derived condition.*

Remark 3. *The computational complexity of the proposed condition can be evaluated in terms of the number of decision variables (NDVs). The NDVs of the methods in [19,23,39] are* $126n^2 + 17n + 1$, $118n^2 + 15n + 1$, *and* $13.5n^2 + 10.5n$, *respectively, while the proposed approach involves* $212.5n^2 + 6.5n$ *decision variables. It can be observed that all methods exhibit a similar polynomial growth with respect to the system dimension, i.e., on the order of* $O(n^2)$.

Following the derivation of Theorem 1, setting $w(t) \equiv 0$ leads to $\dot{V}(t) < 0$. Thus, by Lyapunov's stability theory, the following corollary is obtained:

Corollary 1. *If the matrix inequities specified in Theorem 1 are satisfied, then the MBNN in (2.3) with* $w(t) \equiv 0$ *is asymptotically stable.*

4. Controller design

Theorem 2. *For prescribed $\mathcal{H}_\infty$ performance level $\gamma_1 > 0$, $\mathcal{L}_2 - \mathcal{L}_\infty$ performance level $\gamma_2 > 0$, lower bound $\rho_1 > 0$, upper bound $\rho_2 > 0$ of the time-varying delay $\rho(t)$, $\varepsilon_1 > 0$, and $\varepsilon_2 > 0$, assume the existence of $L_1, L_2 \in \mathbb{R}^{n\times n}$, $M_1, M_2 \in \mathbb{R}^{18n\times 2n}$, $\Pi = (\Pi_{jk})_{5\times 5} \in \mathbb{S}_+^{5n}$, $N_1, N_2, W_1, W_2 \in \mathbb{S}_+^n$, positive diagonal matrices $Q_1, Q_2, \Theta_1, \Theta_2, \Theta_3, \Theta_4$, and matrices $Z_1, Z_2 \in \mathbb{R}^{18n\times 3n}$ satisfying (3.2) and*

$$\begin{bmatrix} \tilde{O}_0^i(\varpi, Z) & \varpi Z_1 + (1-\varpi)Z_2 & \Phi_1 & \Phi_2 & \Phi_3 & \Phi_4 & \Phi_5 & \Phi_6 \\ * & -\tilde{W}_2 & 0 & 0 & 0 & 0 & 0 & 0 \\ * & * & -\Theta_1 & 0 & 0 & 0 & 0 & 0 \\ * & * & * & -\Theta_3 & 0 & 0 & 0 & 0 \\ * & * & * & * & -\Theta_2 & 0 & 0 & 0 \\ * & * & * & * & * & -\Theta_4 & 0 & 0 \\ * & * & * & * & * & * & -\varepsilon_1(P+P^T)+\varepsilon_2 I & 0 \\ * & * & * & * & * & * & * & -\varepsilon_2 I \end{bmatrix} < 0 \tag{4.1}$$

for any $\varpi \in \{0, 1\}$, where

$$\tilde{O}_0^i(\varpi, Z) = \tilde{O}_0^i(\varpi) + \kappa_1^T C^T C \kappa_1 + (1-\gamma_1^2)\kappa_{18}^T I \kappa_{18} - \Gamma^T \mathcal{W}_2(\varpi)\Gamma - \mathrm{He}\left(\Gamma^T \begin{bmatrix} (1-\varpi)Z_1^T \\ \varpi Z_2^T \end{bmatrix}\right),$$

$$\tilde{O}_0^i(\varpi) = He\left[(\bar{\kappa}_1^T(\varpi)\Pi\bar{\kappa}_0) + M_1\bar{\rho}_{1,\kappa}(\varpi) + M_2\bar{\rho}_{2,\kappa}(\varpi)\right] + \hat{N} - \bar{\kappa}_2^T\tilde{W}_1\bar{\kappa}_2 + \hat{U}$$

$$
\begin{aligned}
&+ 2\kappa_1^T(-L_1^T - D^T L_2)\kappa_{15} + 2\kappa_1^T(L_1^T A_0 + Q_1\Psi)\kappa_{16} \\
&+ 2\kappa_{15}^T L_2^T A_0\kappa_{16} + 2\kappa_1^T L_1^T A_{d0}\kappa_{17} + 2\kappa_{15}^T L_2^T A_{d0}\kappa_{17} + 2\kappa_3^T Q_2\Psi\kappa_{17} \\
&+ 2\kappa_1^T L_1^T E\kappa_{18} + 2\kappa_{15}^T L_2^T E\kappa_{18} - \kappa_{18}^T\kappa_{18} + 2\kappa_1^T BF_0VC\kappa_1 + 2\kappa_1^T(BF_0VC)^T\kappa_{15}, \\
\hat{U} &= diag\{He(-L_1^T D),\ 0_{13n\times 13n}, He(-L_2^T) + \rho_1^2 W_1 + \rho_{12}^2 W_2, \\
&\quad He(-Q_1) + A_2^T(\Theta_1 + \Theta_2)A_2, He(-Q_2) + A_{d2}^T(\Theta_3 + \Theta_4)A_{d2},\ 0_{n\times n}\}, \\
\Phi_5 &= \begin{bmatrix} F_0^T B^T L_1 - P^T F_0^T B^T + \varepsilon_1 VC & 0_{n\times 13n} & F_0^T B^T L_2 - P^T F_0^T B^T & 0_{n\times 3n} \end{bmatrix}^T, \\
\Phi_6 &= \begin{bmatrix} F_1^T B^T L_1 & 0_{n\times 13n} & F_1^T B^T L_2 & 0_{n\times 3n} \end{bmatrix}^T,
\end{aligned}
$$

and the other notations employed are consistent with those in Theorem 1. Then, MBNN (2.3) possesses both $\mathcal{H}_\infty$ and $\mathcal{L}_2 - \mathcal{L}_\infty$ disturbance attenuation if the controller gain is designed as

$$K = P^{-1}V. \tag{4.2}$$

Proof. The core of the proof lies in showing that the feasibility of the condition in (4.1) ensures the satisfaction of (3.1) under the proposed control law. To maintain conciseness and avoid redundant algebraic manipulations, we focus on the pivotal transformation steps. The matrix inequality originally expressed in (3.1) can be equivalently reformulated as follows:

$$\Omega_1 + \mathrm{He}\left(\Delta_{B,L}(F_0 + F_1\lambda)K\Delta_C\right) < 0, \tag{4.3}$$

where

$$
\begin{aligned}
\Omega_1 &= \begin{bmatrix} \tilde{O}_0^i(\varpi, Z) & \varpi Z_1 + (1-\varpi)Z_2 & \Phi_1 & \Phi_2 & \Phi_3 & \Phi_4 \\ * & -\tilde{W}_2 & 0 & 0 & 0 & 0 \\ * & * & -\Theta_1 & 0 & 0 & 0 \\ * & * & * & -\Theta_3 & 0 & 0 \\ * & * & * & * & -\Theta_2 & 0 \\ * & * & * & * & * & -\Theta_4 \end{bmatrix}, \\
\Delta_{B,L} &= \begin{bmatrix} B^T L_1 & 0_{n\times 13n} & B^T L_2 & 0_{n\times 11n} \end{bmatrix}^T, \\
\Delta_C &= [C \ \ 0_{n\times 25n}].
\end{aligned}
$$

By substituting (4.2) into (4.3), the original nonlinear term can be decomposed into a nominal part and an uncertainty-related remainder as

$$
\begin{aligned}
\Delta_{B,L}(F_0 + F_1\lambda)K\Delta_C &= \begin{bmatrix} L_1^T B \\ 0_{13n\times n} \\ L_2^T B \\ 0_{11n\times n} \end{bmatrix}(F_0 + F_1\lambda)P^{-1}V[C\ 0_{n\times 25n}] = \begin{bmatrix} L_1^T B(F_0 + F_1\lambda)P^{-1}VC & 0_{n\times 25n} \\ 0_{13n\times n} & 0_{13n\times 25n} \\ L_2^T B(F_0 + F_1\lambda)P^{-1}VC & 0_{n\times 25n} \\ 0_{11n\times n} & 0_{11n\times 25n} \end{bmatrix} \\
&= \begin{bmatrix} BF_0VC + (L_1^T B(F_0 + F_1\lambda) - BF_0P)P^{-1}VC & 0_{n\times 25n} \\ 0_{13n\times n} & 0_{13n\times 25n} \\ BF_0VC + (L_2^T B(F_0 + F_1\lambda) - BF_0P)P^{-1}VC & 0_{n\times 25n} \\ 0_{11n\times n} & 0_{3n\times 25n} \end{bmatrix}.
\end{aligned}
$$

To facilitate the separation of the linear term involving V, let us define an auxiliary matrix Δ_B and compute the product $\Delta_B F_0 V \Delta_C$:

$$\Delta_B = \begin{bmatrix} B \\ 0_{13n\times n} \\ B \\ 0_{11n\times n} \end{bmatrix},\ \Delta_B F_0 V \Delta_C = \begin{bmatrix} BF_0VC & 0_{n\times 25n} \\ 0_{13n\times n} & 0_{13n\times 25n} \\ BF_0VC & 0_{n\times 25n} \\ 0_{11n\times n} & 0_{11n\times 25n} \end{bmatrix}.$$

Meanwhile, calculating the product involving the matrix difference $(\Delta_{B,L}(F_0 + F_1\lambda) - \Delta_B F_0 P)$ leads to the following expression:

$$\begin{aligned}(\Delta_{B,L}(F_0 + F_1\lambda) - \Delta_B F_0 P)P^{-1}V\Delta_C &= \left(\begin{bmatrix} L_1^T B \\ 0_{13n\times n} \\ L_2^T B \\ 0_{11n\times n} \end{bmatrix}(F_0 + F_1\lambda) - \begin{bmatrix} B \\ 0_{13n\times n} \\ B \\ 0_{11n\times n} \end{bmatrix} F_0 P\right) P^{-1}V[C\ 0_{n\times 25n}] \\ &= \begin{bmatrix} (L_1^T B(F_0 + F_1\lambda) - BF_0P)P^{-1}VC & 0_{n\times 25n} \\ 0_{13n\times n} & 0_{13n\times 25n} \\ (L_2^T B(F_0 + F_1\lambda) - BF_0P)P^{-1}VC & 0_{n\times 25n} \\ 0_{11n\times n} & 0_{11n\times 25n} \end{bmatrix}.\end{aligned}$$

Based on the above derivations, the term $\Delta_{B,L}(F_0 + F_1\lambda)K\Delta_C$ can be perfectly reconstructed as:

$$\Delta_{B,L}(F_0 + F_1\lambda)K\Delta_C = \Delta_B F_0 V\Delta_C + (\Delta_{B,L}(F_0 + F_1\lambda) - \Delta_B F_0 P)P^{-1}V\Delta_C, \tag{4.4}$$

where the first term is linear, while the second term contains the residual coupling caused by the fault uncertainty and the matrix P. In view of (4.4), we can re-express (4.3) as

$$\Omega_1 + \mathrm{He}(\Delta_B F_0 V\Delta_C + (\Delta_{B,L}(F_0 + F_1\lambda) - \Delta_B F_0 P)P^{-1}V\Delta_C) < 0. \tag{4.5}$$

We denote

$$\bar{\Phi}_5 = \left[(F_0 + F_1\lambda)^T B^T L_1 - P^T F_0^T B^T + \varepsilon_1 VC\ \ 0_{n\times 13n}\ \ (F_0 + F_1\lambda)^T B^T L_2 - P^T F_0^T B^T\ \ 0_{n\times 3n}\right]^T.$$

Then, by Lemma 5, (4.5) is inherently satisfied if the following holds:

$$\begin{bmatrix} \tilde{O}_0^i(\varpi, Z) & \varpi Z_1 + (1-\varpi)Z_2 & \Phi_1 & \Phi_2 & \Phi_3 & \Phi_4 & \bar{\Phi}_5 \\ * & -\tilde{W}_2 & 0 & 0 & 0 & 0 & 0 \\ * & * & -\Theta_1 & 0 & 0 & 0 & 0 \\ * & * & * & -\Theta_3 & 0 & 0 & 0 \\ * & * & * & * & -\Theta_2 & 0 & 0 \\ * & * & * & * & * & -\Theta_4 & -\varepsilon_1(P + P^T) \end{bmatrix} < 0.$$

This condition can be equivalently written as

$$\Omega_2 = \begin{bmatrix} \tilde{O}_0^i(\varpi, Z) & \varpi Z_1 + (1-\varpi)Z_2 & \Phi_1 & \Phi_2 & \Phi_3 & \Phi_4 & \Phi_5 \\ * & -\tilde{W}_2 & 0 & 0 & 0 & 0 & 0 \\ * & * & -\Theta_1 & 0 & 0 & 0 & 0 \\ * & * & * & -\Theta_3 & 0 & 0 & 0 \\ * & * & * & * & -\Theta_2 & 0 & 0 \\ * & * & * & * & * & -\Theta_4 & -\varepsilon_1(P + P^T) \end{bmatrix} + \mathrm{He}(\Delta_\psi \lambda \Delta_\xi) < 0, \tag{4.6}$$

where

$$\Delta_\psi = \left[F_1^T B^T L_1 \;\; 0_{n\times 13n} \;\; F_1^T B^T L_2 \;\; 0_{n\times 12n}\right]^T,$$
$$\Delta_\xi = \left[0_{n\times 26n} \;\; 1_{n\times n}\right].$$

Noting $\lambda^T\lambda \le I$, by Lemma 3, (4.6) holds true if the following inequality is satisfied:

$$\Omega_2 + \varepsilon_2^{-1}\Delta_\psi\Delta_\psi^T + \varepsilon_2\Delta_\xi^T\Delta_\xi < 0,$$

which, by Lemma 4, can be re-organized as (4.1). The proof of the theorem is hereby complete. □

Remark 4. *Theorem 2 provides a feasible synthesis condition for the fault-resilient output-feedback controller. In contrast, Theorem 1 only gives a sufficient condition to guarantee the dual $\mathcal{H}_\infty$ and $\mathcal{L}_2 - \mathcal{L}_\infty$ performance for the considered delayed MBNN with actuator faults when the controller gain K is known. However, due to the presence of nonlinear coupling terms, the main inequality involved in the condition is nonconvex and thus not amenable to a direct solution. By introducing suitable inequalities together with the lemmas, Theorem 2 transforms the nonlinear inequality into a linear matrix inequality (LMI), facilitating the computation of the controller gain. This enables a tractable controller synthesis procedure.*

5. Numerical example

The following simulation example demonstrates the practical feasibility of the designed output-feedback controller, alongside the theoretical $\mathcal{H}_\infty$ and $\mathcal{L}_2 - \mathcal{L}_\infty$ performance guarantees for delayed MBNNs experiencing actuator faults and external disturbances.

5.1. Simulation setup and parameter selection

Let us examine a two-dimensional MBNN described by (2.1). The activation functions are selected as $\varsigma(\eta_j(t)) = \tanh(\eta_j(t))$ for $j = 1, 2$, fulfilling the condition in (2.6) with $\Psi = diag\{1, 1\}$. The system parameters are chosen based on [23]:

$$D(\eta(t)) = \begin{bmatrix} d_1(\eta_1(t)) & 0 \\ 0 & d_2(\eta_2(t)) \end{bmatrix},$$

$$A(\eta(t)) = \begin{bmatrix} a_{11}(\eta_1(t)) & 0.6 \\ 0.5 & a_{22}(\eta_2(t)) \end{bmatrix},\; A_d(\eta(t)) = \begin{bmatrix} -0.1 & a_{d12}(\eta_1(t)) \\ a_{d21}(\eta_2(t)) & -0.2 \end{bmatrix},$$

where

$$d_1(\eta_1(t)) = \begin{cases} 1, & |\eta_1(t)| \le 0.5, \\ 0.9, & |\eta_1(t)| > 0.5, \end{cases} \quad d_2(\eta_2(t)) = \begin{cases} 0.9, & |\eta_2(t)| \le 0.5, \\ 1, & |\eta_2(t)| > 0.5, \end{cases}$$

$$a_{11}(\eta_1(t)) = \begin{cases} 0, & |\eta_1(t)| \le 0.5, \\ -0.1, & |\eta_1(t)| > 0.5, \end{cases} \quad a_{22}(\eta_2(t)) = \begin{cases} -0.1, & |\eta_2(t)| \le 0.5, \\ 0, & |\eta_2(t)| > 0.5, \end{cases}$$

$$a_{d12}(\eta_1(t)) = \begin{cases} 0.6, & |\eta_1(t)| \le 0.5, \\ 0.1, & |\eta_1(t)| > 0.5, \end{cases} \quad a_{d21}(\eta_2(t)) = \begin{cases} 0.3, & |\eta_2(t)| \le 0.5, \\ 0.2, & |\eta_2(t)| > 0.5, \end{cases}$$

$$w(t) = \begin{bmatrix} 1.8e^{-0.5t} & 1.8e^{-0.5t} \end{bmatrix}, \rho(t) = 1 + 3|\sin(t)|,$$
$$D = \begin{bmatrix} 0.95 & 0 \\ 0 & 0.95 \end{bmatrix}, B = \begin{bmatrix} 4 & 2 \\ 1 & 3 \end{bmatrix}, E = \begin{bmatrix} 0.1 & 0.2 \\ 0.3 & 0.4 \end{bmatrix}, C = \begin{bmatrix} 1 & 2 \\ 1 & 2 \end{bmatrix},$$
$$\hat{F} = \begin{bmatrix} 1.0 & 0 \\ 0 & 0.9 \end{bmatrix}, \check{F} = \begin{bmatrix} 0.6 & 0 \\ 0 & 0.7 \end{bmatrix},$$

from which we can write

$$A_0 = \begin{bmatrix} -0.05 & 0.6 \\ 0.5 & -0.05 \end{bmatrix}, A_{d0} = \begin{bmatrix} -0.1 & 0.35 \\ 0.25 & -0.2 \end{bmatrix},$$
$$A_1 = \begin{bmatrix} \sqrt{0.05} & 0 & 0 & 0 \\ 0 & 0 & 0 & \sqrt{0.05} \end{bmatrix}, A_2^T = \begin{bmatrix} \sqrt{0.05} & 0 & 0 & 0 \\ 0 & 0 & 0 & \sqrt{0.05} \end{bmatrix},$$
$$A_{d1} = \begin{bmatrix} 0 & \sqrt{0.25} & 0 & 0 \\ 0 & 0 & \sqrt{0.05} & 0 \end{bmatrix}, A_{d2}^T = \begin{bmatrix} 0 & 0 & \sqrt{0.05} & 0 \\ 0 & \sqrt{0.25} & 0 & 0 \end{bmatrix},$$
$$F_0 = \begin{bmatrix} 0.8 & 0 \\ 0 & 0.8 \end{bmatrix}, F_1 = \begin{bmatrix} 0.2 & 0 \\ 0 & 0.1 \end{bmatrix}.$$

Table 1. Comparison of maximum allowable delay bound ρ_2 (time in seconds) for various lower delay bounds ρ_1 (time in seconds) under the unified performance setting $\gamma_1 = \gamma_2$.

$\gamma_1 = \gamma_2$	Method	ρ_2 for different ρ_1						
		$\rho_1 = 0$	$\rho_1 = 0.5$	$\rho_1 = 1$	$\rho_1 = 1.5$	$\rho_1 = 2$	$\rho_1 = 2.5$	$\rho_1 = 3$
0.4	Theorem 1 of this paper	3.46	3.79	4.10	4.41	4.76	5.17	5.61
	Theorem 1 of [19]	3.11	3.52	3.90	4.26	4.63	5.05	5.49
	Theorem 1 of [23]	2.81	3.22	3.60	3.95	4.31	4.70	5.12
	Theorem 1 of [39]	3.20	3.61	3.98	4.33	4.70	5.12	5.55
0.6	Theorem 1 of this paper	3.73	4.05	4.40	4.72	5.09	5.46	5.88
	Theorem 1 of [19]	3.38	3.79	4.17	4.53	4.90	5.32	5.76
	Theorem 1 of [23]	3.04	3.46	3.85	4.21	4.59	5.01	5.46
	Theorem 1 of [39]	3.20	3.61	3.98	4.33	4.70	5.12	5.55
0.8	Theorem 1 of this paper	3.98	4.34	4.65	4.87	5.26	5.70	6.11
	Theorem 1 of [19]	3.65	4.06	4.44	4.80	5.17	5.59	6.03
	Theorem 1 of [23]	3.25	3.67	4.06	4.42	4.80	5.23	5.68
	Theorem 1 of [39]	3.20	3.61	3.98	4.33	4.70	5.12	5.55

5.2. Comparative analysis of delay bounds

The comparative results presented in Table 1 reveal that the proposed analysis method provides larger maximum allowable bounds ρ_2 than those reported in [19, 23, 39] for all given values of the lower delay bound ρ_1 under the unified performance setting $\gamma_1 = \gamma_2$. Notably, the condition in [19] guarantees only the $\mathcal{H}_\infty$ performance, the condition in [23] considers only the $\mathcal{L}_2 - \mathcal{L}_\infty$ performance, and the

condition in [39] focuses solely on stability analysis without performance constraints. In contrast, the proposed condition simultaneously ensures both $\mathcal{H}_\infty$ and $\mathcal{L}_2 - \mathcal{L}_\infty$ performance specifications under the same system setting. Despite imposing these more stringent dual performance requirements, the derived delay-dependent condition still admits strictly larger allowable delay bounds. As ρ_1 increases, the corresponding allowable upper delay bound ρ_2 increases accordingly, confirming the effectiveness of the proposed condition in handling time-varying delays. Furthermore, as the disturbance-attenuation level γ increases, the corresponding allowable upper delay bound ρ_2 also increases, which is consistent with the fact that less-stringent performance requirements generally lead to less-conservative delay bounds.

5.3. Simulation results and robustness evaluation

In order to clearly demonstrate the effectiveness of the proposed control strategy, the $\mathcal{H}_\infty$ and $\mathcal{L}_2 - \mathcal{L}_\infty$ performance indices are evaluated both before and after the controller is applied. Specifically, the following functions are introduced:

$$H(t) = \left(\frac{\int_0^t y^T(r)y(r)\,dr}{\int_0^\infty w^T(r)w(r)\,dr} \right)^{1/2}, \quad L(t) = \left(\frac{y^T(t)y(t)}{\int_0^\infty w^T(r)w(r)\,dr} \right)^{1/2}.$$

These two functions are employed to assess the $\mathcal{H}_\infty$ and $\mathcal{L}_2 - \mathcal{L}_\infty$ performance in this study, respectively.

We set $\gamma_1 = 0.6, \gamma_2 = 0.8$, and $\eta(s) = [2, 4]^T$, $t \in [-4, 0]$. Then, under a zero control input, the state trajectories are depicted in Figure 1, while the evolutions of $H(t)$ and $L(t)$ are shown in Figures 2 and 3, respectively. It is clearly observed that the unforced trajectories cannot achieve convergence to the equilibrium point, and the prescribed $\mathcal{H}_\infty$ and $\mathcal{L}_2 - \mathcal{L}_\infty$ performance requirements are not met in the absence of control.

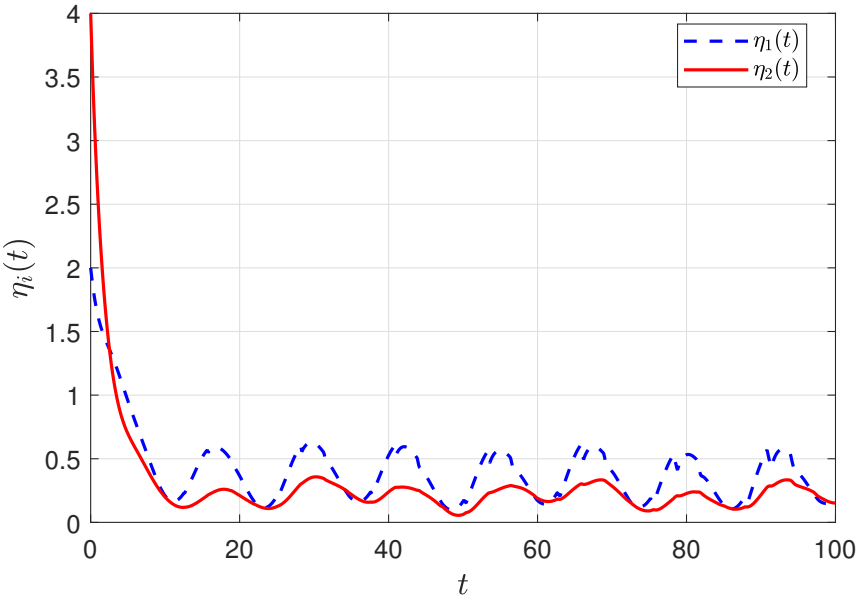

Figure 1. Open-loop state trajectories (time in seconds).

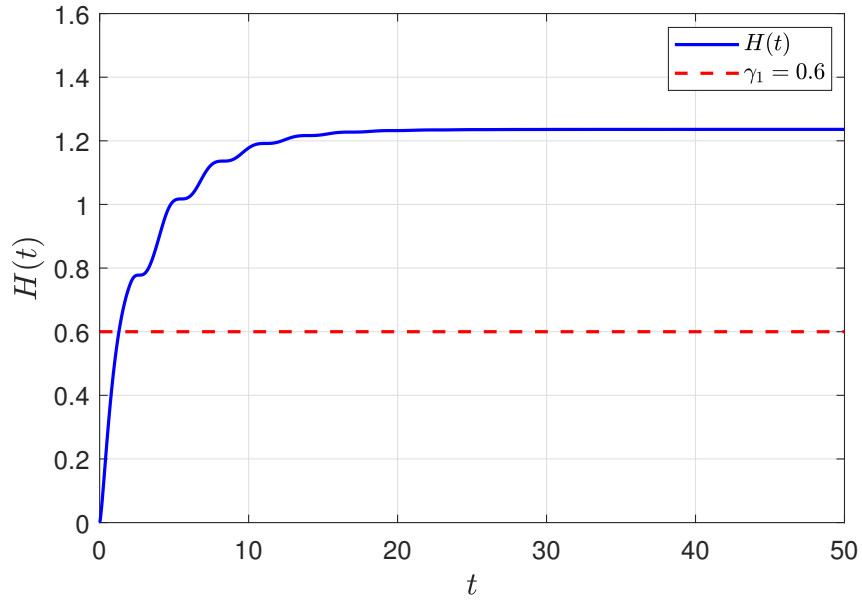

Figure 2. Evolution of $H(t)$ for the open-loop MBNN (time in seconds).

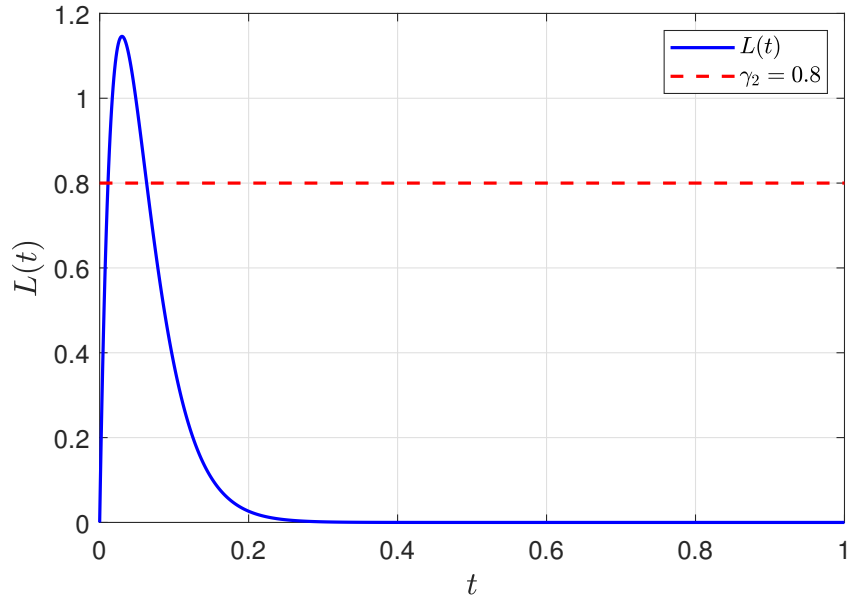

Figure 3. Evolution of $L(t)$ for the open-loop MBNN (time in seconds).

Based on the time-varying delay configuration, the delay bounds are set as $\rho_1 = 1$ and $\rho_2 = 4$. With these prescribed bounds, the LMIs in Theorem 2 are found to be feasible, yielding the following controller gain:

$$K = \begin{bmatrix} -0.7055 & -0.1476 \\ 0.2513 & 0.0664 \end{bmatrix}.$$

By applying control law (2.2) with the above calculated gain, the closed-loop state trajectories and the evolutions of $H(t)$ and $L(t)$ are shown in Figures 4–6. As shown in Figure 4, the proposed control scheme effectively regulates all state variables to the equilibrium point. Figures 5 and 6 further demonstrate that $H(\infty) < 0.6$ and $\sup_{t\geq 0} L(t) < 0.8$, verifying that the proposed controller effectively suppresses the influence of external disturbances and provides dual robust performance guarantees.

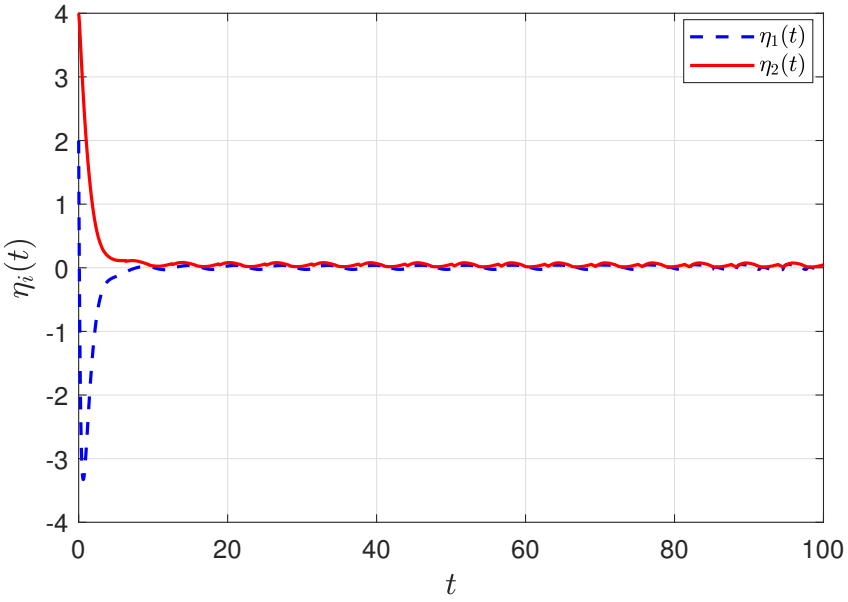

Figure 4. Closed-loop state trajectories (time in seconds).

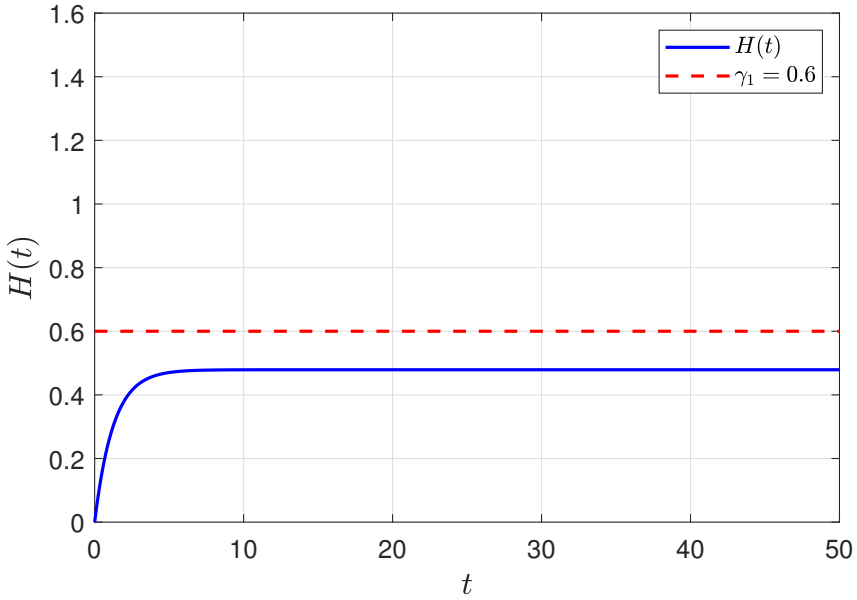

Figure 5. Evolution of $H(t)$ for the closed-loop MBNN with $\gamma_1 = 0.6$ (time in seconds).

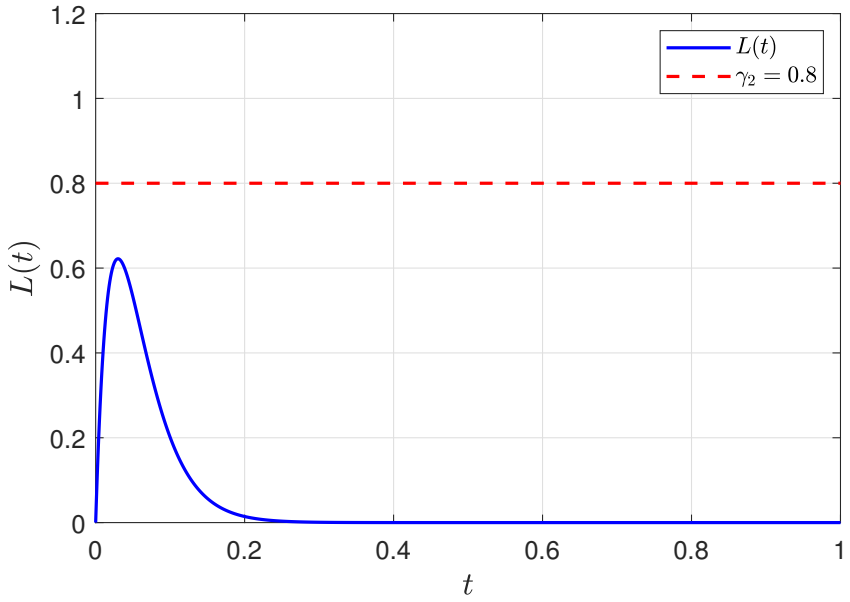

Figure 6. Evolution of $L(t)$ for the closed-loop MBNN with $\gamma_2 = 0.8$ (time in seconds).

Table 2. Comparison of the values of the performance pair $(H(\infty), \sup_{t\geq 0} L(t))$ under different actuator fault factors and disturbance intensities.

Fault level	λ_0	$(H(\infty), \sup_{t\geq 0} L(t))$		
		$e = 0.2$	$e = 0.4$	$e = 0.6$
No fault	0	(0.334, 0.429)	(0.385, 0.482)	(0.454, 0.543)
Moderate fault	0.5	(0.432, 0.550)	(0.485, 0.612)	(0.531, 0.673)
Severe fault	1	(0.503, 0.643)	(0.570, 0.709)	(0.624, 0.768)

To further assess the effectiveness of the proposed control strategy under different actuator faults and external disturbances, the fault matrices and the disturbance matrix are assigned as follows:

$$F_0 = I,\ \lambda = \lambda_0 I, F_1 = \begin{bmatrix} 0.6 & 0 \\ 0 & 0.8 \end{bmatrix},\ E = \begin{bmatrix} 0.1 & 0.2 \\ 0.3 & e \end{bmatrix},$$

where the scalar e characterize the disturbance intensity.

For each combination of f and λ_0 listed in Table 2, the corresponding controller gain K is obtained by solving the conditions in Theorem 2. Then, based on the closed-loop simulations, the performance pair $(H(\infty), \sup_{t\geq 0} L(t))$ is summarized in Table 2. As shown in the table, for a fixed disturbance intensity e, both $H(\infty)$ and $\sup_{t\geq 0} L(t))$ increase as the fault-level coefficient λ_0 becomes larger. This implies that more severe actuator fault degradation leads to a degradation in the disturbance attenuation performance. Nevertheless, the performance indices satisfy $H(\infty) < \gamma_1 = 0.6$ and $\sup_{t\geq 0} L(t) < \gamma_2 = 0.8$ in all considered cases, demonstrating that the controller obtained from Theorem 2 can effectively tolerate actuator faults. Moreover, for a fixed fault level λ_0, increasing e leads to larger values of $H(\infty)$ and $\sup_{t\geq 0} L(t))$, which indicates that stronger external disturbances have a more significant influence on

the system response. These results confirm that the proposed output-feedback controller maintains satisfactory robustness under different actuator fault levels and disturbance intensities.

6. Conclusions

This paper investigates the fault-resilient output-feedback control problem for delayed MBNNs subject to actuator faults and external disturbances. By constructing an appropriate LKF and incorporating the BLI together with the GRCCI, a fault-resilient output-feedback controller is designed via nonlinear decoupling techniques, which successfully transforms the dual $\mathcal{H}_\infty$ and $\mathcal{L}_2 - \mathcal{L}_\infty$ performance requirements into solvable LMIs. A numerical example is provided to validate the proposed approaches. Notably, despite the more stringent dual performance requirements, the derived delay-dependent condition admits a larger allowable upper delay bound than existing methods, indicating the reduced conservatism of the derived analysis result. The simulation results also confirm that the designed controller can not only stabilize delayed MBNNs with actuator faults and external disturbances, but also realize the expected dual robust performance. Future work will focus on event-triggered fault-resilient output-feedback controller designs for more complicated MBNNs, such as stochastic MBNNs and coupling MBNNs.

Use of AI tools declaration

The authors declare they have not used Artificial Intelligence (AI) tools in the creation of this article.

Acknowledgments

This work was supported in part by the Undergraduate Innovation and Entrepreneurship Training Program of Anhui University of Technology (Grant No. S202510360364) and the Natural Science Foundation of Anhui Higher Education Institutions (Grant No. 2023AH051128).

Conflict of interest

There are no conflicts of interest that the author needs to declare regarding the research presented herein.

References

1. G. Tian, Y. Yang, S. Wen, Time-series stock price forecasting based on neural networks: A comprehensive survey, *Artif. Intell. Sci. Eng.*, **1** (2025), 255–277. https://doi.org/10.23919/AISE.2025.000018
2. Q. Liu, H. Yan, H. Zhang, L. Zeng, C. Chen, Adaptive intermittent pinning control for synchronization of delayed nonlinear memristive neural networks with reaction–diffusion items, *IEEE Trans. Neural Networks Learn. Syst.*, **36** (2024), 2234–2245. https://doi.org/10.1109/TNNLS.2023.3344515
3. X. Geng, J. Feng, Y. Zhao, N. Li, J. Wang, Fixed-time synchronization of nonlinear coupled memristive neural networks with time delays via sliding-mode control, *Electron. Res. Arch.*, **31** (2023), 3291–3308. https://doi.org/10.3934/era.2023166

4. Y. Fan, X. Huang, Z. Wang, Memory-dependent event-trigger scheme for secure control of memristive neural networks: Dealing with deception attacks, *IEEE Trans. Ind. Inf.*, **20** (2023), 5562–5571. https://doi.org/10.1109/TII.2023.3335996
5. X. Zhang, J. Lu, Z. Wang, R. Wang, J. Wei, T. Shi, et al., Hybrid memristor-CMOS neurons for in-situ learning in fully hardware memristive spiking neural networks, *Sci. Bull.*, **66** (2021), 1624–1633. https://doi.org/10.1016/j.scib.2021.04.014
6. H. Lin, C. Wang, Q. Hong, Y. Sun, A multi-stable memristor and its application in a neural network, *IEEE Trans. Circuits Syst. II, Exp. Briefs*, **67** (2020), 3472–3476. https://doi.org/10.1109/TCSII.2020.3000492
7. E. Wang, B. Hu, Z. H. Guan, Chaotic dynamics and synchronization of multi-region neural network based on locally active memristor, *Chaos, Solitons Fractals*, **197** (2025), 116437. https://doi.org/10.1016/j.chaos.2025.116437
8. L. Yang, J. Zhang, Memristor-coupled heterogeneous Hopfield neural network with switchable activation functions and its synchronization control, *Chaos, Solitons Fractals*, **200** (2025), 117101. https://doi.org/10.1016/j.chaos.2025.117101
9. S. G. Hu, Y. Liu, Z. Liu, T. P. Chen, J. J. Wang, Q. Yu, et al., Associative memory realized by a reconfigurable memristive Hopfield neural network, *Nat. Commun.*, **6** (2015), 7522. https://doi.org/10.1038/ncomms8522
10. C. Xu, M. Liao, C. Wang, J. Sun, H. Lin, Memristive competitive Hopfield neural network for image segmentation application, *Cogn. Neurodyn.*, **17** (2023), 1061–1077. https://doi.org/10.1007/s11571-022-09891-2
11. S. A. Thomas, R. Sharma, D. M. Das, Analyzing the impact of parasitics on a CMOS-memristive crossbar neural network based on winner-take-all and Hebbian rule, *Mem.-Mater. Devices Circuits Syst.*, **5** (2023), 100081. https://doi.org/10.1016/j.memori.2023.100081
12. S. Zhang, X. Peng, X. Wang, C. Chen, Z. Zeng, A novel memristive multiscroll multistable neural network with application to secure medical image communication, *IEEE Trans. Circuits Syst. Video Technol.*, **35** (2024), 1774–1786. https://doi.org/10.1109/TCSVT.2024.3483569
13. H. Peng, L. Gan, X. Guo, Memristor-based spiking neural networks: Cooperative development of neural network architecture/algorithms and memristors, *Chip*, **3** (2024), 100093. https://doi.org/10.1016/j.chip.2024.100093
14. Z. Yan, X. Huang, J. Liang, Aperiodic sampled-data control for stabilization of memristive neural networks with actuator saturation: A dynamic partitioning method, *IEEE Trans. Cybern.*, **53** (2022), 1725–1737. https://doi.org/10.1109/TCYB.2021.3108805
15. Z. Wang, L. Yan, Y. Fan, F. Wang, H. Shen, Switching event-triggered-based gain-scheduled control for bipartite synchronization of coupled coopetitive memristive neural networks, *IEEE Trans. Syst. Man Cybern. Syst.*, **55** (2025), 6951–6963. https://doi.org/10.1109/TSMC.2025.3594542
16. X. Si, Z. Wang, X. Huang, M. Xiao, Finite-time bipartite synchronization of delayed antagonistic memristive neural networks: Optimizing event-triggered controller parameters, *IEEE Trans. Artif. Intell.*, 2026. https://doi.org/10.1109/TAI.2025.3650558

17. Z. Yang, B. Zhao, D. Liu, Synchronization of delayed memristor-based neural networks via pinning control with local information, *IEEE Trans. Neural Networks Learn. Syst.*, **35** (2023), 13619–13630. https://doi.org/10.1109/TNNLS.2023.3270345

18. C. Yang, J. Wu, Z. Qiao, An improved fixed-time stabilization problem of delayed coupled memristor-based neural networks with pinning control and indefinite derivative approach, *Electron. Res. Arch.*, **31** (2023), 2428–2446. https://doi.org/10.3934/era.2023123

19. Z. Yan, D. Zuo, T. Guo, J. Zhou, Quantized $\mathcal{H}_\infty$ stabilization for delayed memristive neural networks, *Neural Comput. Appl.*, **35** (2023), 16473–16486. https://doi.org/10.1007/s00521-023-08510-3

20. S. Lin, X. Liu, Y. Huang, Event-triggered synchronization and $\mathcal{H}_\infty$ synchronization of coupled delayed reaction-diffusion memristive neural networks, *Math. Methods Appl. Sci.*, **46** (2023), 9079–9102. https://doi.org/10.1002/mma.9039

21. Y. Huang, A. Li, General decay anti-synchronization and $\mathcal{H}_\infty$ anti-synchronization of derivative coupled delayed memristive neural networks with constant and delayed state coupling, *Commun. Nonlinear Sci. Numer. Simul.*, **139** (2024), 108313. https://doi.org/10.1016/j.cnsns.2024.108313

22. J. Wang, T. Ru, H. Shen, J. Cao, J. H. Park, Finite-time $\mathcal{L}_2$–$\mathcal{L}_\infty$ synchronization for semi-Markov jump inertial neural networks using sampled data, *IEEE Trans. Network Sci. Eng.*, **8** (2020), 163–173. https://doi.org/10.1109/TNSE.2020.3032025

23. J. Wang, Y. Zhu, $\mathcal{L}_2$–$\mathcal{L}_\infty$ control for memristive NNs with non-necessarily differentiable time-varying delay, *Math. Biosci. Eng.*, **20** (2023), 13182–13199. https://doi.org/10.3934/mbe.2023588

24. Z. Xu, J. Ren, X. Zhou, J. Yao, Adaptive prescribed performance output feedback control for full-state-constrained DC motors subject to uncertainties and input saturation, *Eur. J. Control*, **77** (2024), 100961. https://doi.org/10.1016/j.ejcon.2024.100961

25. W. Zhang, G. Zong, B. Niu, X. Zhao, N. Xu, Adaptive fuzzy dynamic event-triggered control for PDE-ODE cascaded systems with actuator failures, *Fuzzy Sets Syst.*, **519** (2025), 109514. https://doi.org/10.1016/j.fss.2025.109514

26. D. Grande, A. Peruffo, G. Salavasidis, E. Anderlini, D. Fenucci, A. B. Phillips, et al., Passive fault-tolerant augmented neural Lyapunov control: A method to synthesise control functions for marine vehicles affected by actuators faults, *Control Eng. Pract.*, **148** (2024), 105935. https://doi.org/10.1016/j.conengprac.2024.105935

27. J. Zhang, H. Xia, Y. Zhu, Y. Fu, Research on sensor fault tolerance technology in nuclear power plant control system, *Ann. Nucl. Energy*, **207** (2024), 110714. https://doi.org/10.1016/j.anucene.2024.110714

28. P. Zhu, S. Jin, X. Bu, Z. Hou, Distributed data-driven event-triggered fault-tolerant control for a connected heterogeneous vehicle platoon with sensor faults, *IEEE Trans. Intell. Transp. Syst.*, **25** (2023), 5498–5509. https://doi.org/10.1109/TITS.2023.3335227

29. F. Jia, F. Cao, X. He, Active fault-tolerant control against intermittent faults for state-constrained nonlinear systems, *IEEE Trans. Syst. Man Cybern. Syst.*, **54** (2024), 2389–2401. https://doi.org/10.1109/TSMC.2023.3344292

30. X. Liu, Z. Yuan, Z. Gao, W. Zhang, Reinforcement learning-based fault-tolerant control for quadrotor UAVs under actuator fault, *IEEE Trans. Ind. Inf.*, **20** (2024), 13926–13935. https://doi.org/10.1109/TII.2024.3438241

31. J. Zhou, X. Ma, Z. Yan, C. K. Ahn, Fault-tolerant reduced-order asynchronous networked filtering of $2-D$ Bernoulli jump systems, *IEEE Trans. Syst. Man Cybern. Syst.*, **54** (2023), 891–902. https://doi.org/10.1109/TSMC.2023.3321047

32. Y. Liu, X. Zhao, J. H. Park, F. Fang, Fault-tolerant control for TS fuzzy systems with an aperiodic adaptive event-triggered sampling, *Fuzzy Sets Syst.*, **452** (2023), 23–41. https://doi.org/10.1016/j.fss.2022.04.019

33. J. Liu, J. Dong, Fault-tolerant consensus control with privacy-preserving virtual layer for heterogeneous multi-agent system, *IEEE Trans. Autom. Sci. Eng.*, **22** (2024), 5687–5699. https://doi.org/10.1109/TASE.2024.3428408

34. Z. Du, Y. Lyu, Z. Wu, J. Zhu, Z. Liu, Y. Yang, Fault-tolerant control based on dynamic regressor extension and mixing and adaptive allocation for fixed-wing aircraft with asymmetric damage, *IEEE Trans. Aerosp. Electron. Syst.*, **61** (2025), 9774–9789. https://doi.org/10.1109/TAES.2025.3558180

35. M. Jamali, H. R. Baghaee, M. S. Sadabadi, G. B. Gharehpetian, A. Anvari-Moghaddam, F. Blaabjerg, Distributed finite-time fault-tolerant control of isolated AC microgrids considering input constraints, *IEEE Trans. Smart Grid*, **13** (2022), 4525–4537. https://doi.org/10.1109/TSG.2022.3188199

36. J. Zhou, Y. Liu, J. Xia, Z. Wang, S. Arik, Resilient fault-tolerant anti-synchronization for stochastic delayed reaction–diffusion neural networks with semi-Markov jump parameters, *Neural Networks*, **125** (2020), 194–204. https://doi.org/10.1016/j.neunet.2020.02.015

37. D. Chen, K. Shi, O. Kwon, X. Cai, Y. Sun, S. Wen, et al., Fault-tolerant impulsive synchronization in hypercomplex neural networks via AI-driven adaptive switching mechanism, *Commun. Nonlinear Sci. Numer. Simul.*, **153** (2026), 109511. https://doi.org/10.1016/j.cnsns.2025.109511

38. T. Radhika, A. Chandrasekar, Y. C. Lee, A. R. Subhashri, M. A. Shamrooz, W. J. Chang, Fault-tolerant state estimation synthesis for competitive neural networks subject to deception attacks using probabilistic time varying delay, *J. Franklin Inst.*, **363** (2026), 108679. https://doi.org/10.1016/j.jfranklin.2026.108679

39. Z. Du, J. Zhu, H. Wang, Stability criteria for memristor-based generalized neural networks with time-varying delay via an improved integral inequality, *Nonlinear Dyn.*, **113** (2025), 1745–1759. https://doi.org/10.1007/s11071-024-10313-7

40. G. Chen, J. Xia, J. H. Park, H. Shen, G. Zhuang, Sampled-data synchronization of stochastic Markovian jump neural networks with time-varying delay, *IEEE Trans. Neural Netw. Learn. Syst.*, **33** (2022), 3829–3841. https://doi.org/10.1109/TNNLS.2021.3054615

41. G. Zhuang, J. Xia, J. E. Feng, Y. Wang, G. Chen, Dynamic compensator design and $\mathcal{H}_\infty$ admissibilization for delayed singular jump systems via Moore–Penrose generalized inversion technique, *Nonlinear Anal. Hybrid Syst.*, **49** (2023), 101361. https://doi.org/10.1016/j.nahs.2023.101361

42. J. Zhou, X. Ma, Z. Yan, S. Arik, Non-fragile output-feedback control for time-delay neural networks with persistent dwell time switching: A system mode and time scheduler dual-dependent design, *Neural Networks*, **169** (2024), 733–743. https://doi.org/10.1016/j.neunet.2023.11.007

43. S. Zhao, L. Zhao, S. Wen, L. Cheng, Secure synchronization control of Markovian jump neural networks under DoS attacks with memory-based adaptive event-triggered mechanism, *Artif. Intell. Sci. Eng.*, **1** (2025), 64–78. https://doi.org/10.23919/AISE.2025.000006

44. R. Zhang, H. Wang, J. H. Park, P. He, X. Xie, Event-triggered impulsive fault-tolerant control for memristor-based RDNNs with actuator faults, *IEEE Trans. Neural Netw. Learn. Syst.*, **34** (2023), 2993–3004. https://doi.org/10.1109/TNNLS.2021.3110756

45. L. Feng, D. Li, C. Zhang, Y. Yang, Note on control for hybrid stochastic systems by intermittent feedback rooted in discrete observations of state and mode with delays, *Electron. Res. Arch.*, **32** (2024), 17–40. https://doi.org/10.3934/era.2024002

46. X. Han, Y. Yu, X. Wang, J. Cai, X. Feng, J. Wang, et al., Fault-tolerant bumpless transfer control for fuzzy switched delayed memristive neural networks subject to false data injection attacks, *Chaos Solitons Fractals*, **193** (2025), 116080. https://doi.org/10.1016/j.chaos.2025.116080

47. Z. Yan, X. Huang, Y. Fan, J. Xia, H. Shen, Threshold-function-dependent quasi-synchronization of delayed memristive neural networks via hybrid event-triggered control, *IEEE Trans. Syst. Man Cybern. Syst.*, **51** (2020), 6712–6722. https://doi.org/10.1109/TSMC.2020.2964605

48. Y. Xin, Y. Wang, L. Mu, Z. Cheng, Stability criteria of delayed memristor-based neural networks via continuous-time model and interval matrix approach, *IEEE Trans. Syst. Man Cybern. Syst.*, **53** (2022), 2716–2725. https://doi.org/10.1109/TSMC.2022.3218347

49. B. Li, L. Zhao, S. Wen, Periodic event-triggered consensus of stochastic multi-agent systems under switching topology, *Artif. Intell. Sci. Eng.*, **1** (2025), 147–156. https://doi.org/10.23919/AISE.2025.000011

50. M. Solak, O. Faydasicok, S. Arik, A general framework for robust stability analysis of neural networks with discrete time delays, *Neural Networks*, **162** (2023), 186–198. https://doi.org/10.1016/j.neunet.2023.02.040

51. Y. Cui, P. Cheng, Exponential synchronization of stochastic time-delayed memristor-based neural networks via pinning impulsive control, *Int. J. Control Autom. Syst.*, **22** (2024), 2283–2292. https://doi.org/10.1007/s12555-022-1090-8

52. Q. Song, Q. Wu, Y. Liu, Stabilization of chaotic quaternion-valued neutral-type neural networks via sampled-data control with two-sided looped functional approach, *Nonlinear Anal. Model. Control*, **29** (2024), 1150–1166. https://doi.org/10.15388/namc.2024.29.37852

53. L. He, X. Zhang, T. Jiang, C. Tang, Guaranteed performance control for delayed Markov jump neural networks with output quantization and data-injection attacks, *Int. J. Mach. Learn. Cybern.*, **16** (2025), 173–188. https://doi.org/10.1007/s13042-024-02195-3

54. A. Seuret, F. Gouaisbaut, Hierarchy of LMI conditions for the stability analysis of time-delay systems, *Syst. Control Lett.*, **81** (2015), 1–7. https://doi.org/10.1016/j.sysconle.2015.03.007

55. A. Seuret, K. Liu, F. Gouaisbaut, Generalized reciprocally convex combination lemmas and its application to time-delay systems, *Automatica*, **95** (2018), 488–493. https://doi.org/10.1016/j.automatica.2018.06.017

56. Y. Wang, L. Xie, C. E. De Souza, Robust control of a class of uncertain nonlinear systems, *Syst. Control Lett.*, **19** (1992), 139–149. https://doi.org/10.1016/0167-6911(92)90097-C

57. S. Boyd, L. El Ghaoui, E. Feron, V. Balakrishnan, *Linear Matrix Inequalities in System and Control Theory*, SIAM, Philadelphia, 1994. https://doi.org/10.1137/1.9781611970777

58. J. Zhou, J. Dong, S. Xu, C. K. Ahn, Input-to-state stabilization for Markov jump systems with dynamic quantization and multimode injection attacks, *IEEE Trans. Syst. Man Cybern. Syst.*, **54** (2024), 2517–2529. https://doi.org/10.1109/TSMC.2023.3344869

59. Y. He, Q. Wang, L. Xie, C. Lin, Further improvement of free-weighting matrices technique for systems with time-varying delay, *IEEE Trans. Autom. Control*, **52** (2007), 293–299. https://doi.org/10.1109/TAC.2006.887907

60. K. Liu, A. Seuret, Y. Xia, Stability analysis of systems with time-varying delays via the second-order Bessel–Legendre inequality, *Automatica*, **76** (2017), 138–142. https://doi.org/10.1016/j.automatica.2016.11.001

AIMS Press